JOURNAL OF PROPULSION AND POWER
Vol. 20, No. 1, January–February 2004

Designing and Testing a Lighter, Simpler, Less-Expensive Liquid-Propellant Pump

Andrew Knight*
Andrew Knight Space Propulsion, Vienna, Virginia 22181

Current turbopump-based rocket-engine technology suffers from high cost and complexity, whereas pressurant-based rocket-engine technology suffers from the substantial weight of high-pressure propellant tanks. A new propellant pressurizer that solves these problems has been designed, built, and successfully tested. The pressurizer consists of three parts: a rotating cylindrical spindle containing a plethora of small transfer chambers, each transfer chamber acting as an individual pressure vessel and configured to fill with propellant at low pressure and drain propellant to the engine combustion chamber under the action of a high-pressure pressurant; and top and bottom chamber separators, each having a filling hole and a draining hole, the filling and draining holes aligned to create a filling and draining region between the chamber separators. The spindle is sandwiched with a good seal between the chamber separators such that, as the spindle rotates, each transfer chamber fills with propellant under low pressure in the filling region and subsequently drains of propellant under high pressure in the draining region. The successful test of the prototype demonstrated the ability of the design to match the performance of current turbopump-based systems at a fraction of the cost and weight.

Nomenclature

A_c	=	cross-sectional area
A_d	=	drain area
A_f	=	fill area
A_{HP}	=	cross-sectional area of higher-pressure region of transfer chamber
A_{leakage}	=	leakage area
A_{LP}	=	cross-sectional area of lower-pressure region of transfer chamber
a	=	acceleration
d	=	distance from outer transfer chamber to outer spindle edge (Fig. 9)
F	=	force
F_{all}	=	allowable material strength
f_{direct}	=	direct leakage fraction
f_e	=	pressurant mass equivalence factor
f_{HP}	=	higher-pressure region cross-sectional area fraction
f_{indirect}	=	indirect leakage fraction
f_{LP}	=	lower-pressure region cross-sectional area fraction
f_{prop}	=	volumetric propellant fraction
f_t	=	tank mass multiplier
g_0	=	gravitational acceleration
I_{sp}	=	specific impulse
L	=	length of each spindle region (Fig. 9)
M_{pres}	=	molecular mass of pressurant
m	=	mass
m_{acc}	=	accumulator mass
m_{bf}	=	rocket booster stage final mass
m_{bi}	=	rocket booster stage initial mass
m_{bp}	=	rocket booster stage propellant mass
m_f	=	rocket final mass after engine burn
m_{friction}	=	additional propellant needed to overcome friction power dissipation
m_{fuelpump}	=	mass of Lanning fuel pump
m_{ggpump}	=	mass of gas generator propellant pump
m_i	=	rocket initial mass
m_{LOXpump}	=	mass of Lanning liquid-oxygen (LOX) pump
$m_{\mathrm{newfuelpump}}$	=	mass of new fuel pump according to the present invention
$m_{\mathrm{newLOXpump}}$	=	mass of new LOX pump according to the present invention
m_{piston}	=	piston mass
m_{pres}	=	pressurant mass
$m_{\mathrm{pres,fixed}}$	=	equivalent fixed pressurant mass
m_{prop}	=	propellant mass
m_{pump}	=	pump mass
m_{spindle}	=	spindle mass
m_{tank}	=	tank mass
$m_{\mathrm{tank,pres}}$	=	pressurant tank mass
m_{ui}	=	rocket upper-stage initial mass
m_{valves}	=	valve mass
$\dot{m}$	=	mass flow rate
$\dot{m}_{\mathrm{direct}}$	=	mass flow rate of pressurant directly leaked from pump
$\dot{m}_{\mathrm{indirect}}$	=	mass flow rate of pressurant indirectly leaked from pump
P	=	pressure
P_b	=	tank burst pressure
P_{final}	=	final pressure in transfer chamber after depressurization
P_{gg}	=	gas generator injector pressure
P_{HP}	=	pressure in higher pressure region of transfer chamber
P_{LP}	=	pressure in lower pressure region of transfer chamber
P_{outlet}	=	pump outlet pressure
Q_{propleak}	=	volumetric propellant leakage rate from pump
R_U	=	universal gas constant
r	=	radius
r_{HP}	=	radius of higher-pressure region of transfer chamber
r_{hex}	=	radius of hexagons in hexagonal transfer chamber configuration
r_{LP}	=	radius of lower-pressure region of transfer chamber
r_r	=	rotation rate
r_1	=	inner radius of spindle
r_2	=	outer radius of spindle

Received 16 January 2003; revision received 24 July 2003; accepted for publication 24 July 2003.

*Proprietor, 2521 Glengyle Dr.; afk3@georgetown.edu. Student Member AIAA.

T_{pres} = pressurant temperature
t = time
t_{burn} = engine burn time
t_{cycle} = cycle time
t_d = drain time
t_{dep} = depressurization time
t_f = fill time
t_{optimum} = cycle time t_{cycle} at which pump mass is minimized
t_{valve} = time required for a valve to fully open or close
V_{prop} = total propellant volume
V_{tank} = tank volume
v = velocity
v_a = acoustic Velocity
v_d = drain velocity
v_f = fill velocity
$\bar{v}_d$ = average drain velocity
$\bar{v}_{\text{dep}}$ = average depressurization velocity
$\bar{v}_f$ = average fill velocity
w_{RMS} = rms width of space between spindle and chamber separators
α_d = radial width of draining region
α_{dep} = radial width of depressurization region
α_f = radial width of filling region
α_{space} = radial width of space/separation region
γ_{pres} = pressurant isentropic parameter
Δm_{direct} = pressurant mass directly leaked from pump
$\Delta m_{\text{indirect}}$ = pressurant mass indirectly leaked from pump
$\Delta m_{\text{leakage}}$ = equivalent leakage mass because of pump
Δm_{pres} = pressurant mass cost because of ΔP_{pres}
Δm_{pump} = equivalent additional pressurant/tank mass because of pump
ΔP_d = pressure drop across the draining region
$\Delta P_{\text{dynamic}}$ = dynamic pressure drop caused by fluid motion
ΔP_f = pressure drop across the filling region
ΔP_{inj} = pressure drop across the gas generator's propellant injector
ΔP_{pres} = pressurant pressure cost because of pump
$\overline{\Delta P}_{\text{dynamic}}$ = average dynamic pressure caused by centrifugal pumping effect
Δv = change in velocity caused by engine burn
μ_{prop} = propellant absolute viscosity
ρ_{piston} = density of piston material
ρ_{pres} = pressurant density
ρ_{prop} = propellant density
ρ_{spindle} = density of spindle material
ϕ_{tank} = tank mass factor

I. Introduction

CURRENTLY, operational launch vehicles are based on turbopump technology from the 1960s. Although turbopumps are well understood and accompanied by many years of test data, the close tolerances of their parts, the exotic nature of their materials, and their extreme complexity cause turbopumps to remain prohibitively expensive for many applications. Relatively recently, there has been a resurgent interest in the free market to substantially reduce per-pound launch costs. Although currently operational vehicles utilize expensive turbopump technology, it is likely that the race for cheap access to space will be won by simpler, more reliable, and less-expensive technology. A new propellant pressurizer design will be described herein.

II. Prior Technology

A. Description of Prior Technology

The choice design of Robert Goddard—because of its simplicity—was a pressurant-based system, in which a gas having a pressure higher than the combustion pressure pushes the propellants into the combustion chamber. The gas can be an inert gas such as nitrogen, the vapor of one of the liquid propellants, or hot gas generated from a gas generator. Further, the gas can be stored in a separate pressurant tank or in the propellant tank itself. On 16 March, 1926, Goddard launched the first liquid-propellant rocket, burning liquid oxygen and gasoline. Liquid-oxygen vapor, created by aiming the hot exhaust gases at the liquid-oxygen tank, was used as the pressurant. A problem with this design—particularly for large-scale and launch applications—is that the propellant tanks must have a wall thickness sufficient to withstand the high pressure and therefore might be prohibitively weighty.

The mass of a spherical propellant tank having a volume V_{tank}, a burst pressure P_b (where P_b is usually twice the maximum expected operating pressure of the tank), and a tank mass factor ϕ_{tank} can be calculated by

$$m_{\text{tank,sphere}} = \frac{P_b V_{\text{tank}}}{\phi_{\text{tank}} g_0} \tag{1}$$

The tank mass factor ϕ_{tank} is approximately 2500 m for completely metallic tanks and can be as high as 10,000 m for fiber-reinforced composite tanks.[1] Similarly, for a spherical tank containing a volumetric fraction f_{prop} of propellant having density ρ_{prop} and pressurized with a light gas to half the tank burst pressure P_b, the ratio of the mass m_{tank} of the tank to the mass m_{prop} of propellant can be calculated by

$$m_{\text{tank}}/m_{\text{prop}} = P_b/\phi_{\text{tank}} g_0 \rho_{\text{prop}} f_{\text{prop}} \tag{2}$$

This calculation neglects the mass of the pressurant, which, as a gas, is substantially lower than the mass of the propellant. For example, assuming a blowdown pressurant system for a hybrid rocket having a single spherical titanium propellant tank filled halfway ($f_{\text{prop}} = 50\%$) with liquid oxygen ($\rho_{\text{LOX}} = 1142$ kg/m^3) and pressurized to 500 psi (3.44 MPa), the mass m_{tank} of the tank is about 49% of the mass m_{prop} of the propellant. A lower tank pressure and the use of stronger, lighter composite materials can further reduce this mass fraction; however, it remains relatively high for pressurant-based systems.

A pump-based system (utilizing, e.g., a turbopump), in place of a pressurant-based system, is capable of substantially reducing this mass fraction because it does not require the propellant tanks to withstand such a high pressure. Rather, the propellant tanks are only pressurized to between 45 and 75 psia (310 kPa and 520 kPa) to provide structure to the tank and to prevent cavitation in the turbopump. The mass "cost" of this benefit is small. A typical turbopump for a rocket vehicle will, itself, weigh only about 0.2–0.4% of the propellant. Further, for a turbopump utilizing a gas generator cycle the energy to drive the turbopump is extracted directly from the propellants, and the rocket must carry an additional 1–2.5% of propellant, with a corresponding drop in I_{sp}. Turbopumps utilizing expander or staged combustion cycles do not require any additional propellant. Although turbopump-based systems help to solve the weight problem imposed by pressurant-based systems, they impose further problems, such as lower reliability and extremely high cost.

The first invention to address the weight problem of pressurant systems while avoiding the need for turbopumps was disclosed in a patent[2] issued in October 1965 to Albert J. Sobey. Sobey recognized that significant mass savings result from reducing the size of those propellant tanks that need to withstand high pressure. Therefore, by pumping the propellant from a large, low-pressure tank to a small tank that is subsequently pressurized to high pressure, only the small tank needs to have walls thick enough to endure the high pressure. Shown in Fig. 1, Sobey's system comprises fuel and oxidizer tanks 22 and 24, a high-pressure gas source 66, a low-pressure gas source 46, two storage tanks 26 and 28 for the fuel tank 22 and two storage tanks 30 and 32 for the oxidizer tank 24, and three reversing valves 50, 52, and 54. Each storage tank has a lower region for propellant and an upper region for high-pressure gas, separated by a membrane 72 to prevent mixing of propellant and high-pressure gas. The fuel and oxidizer tanks 22 and 24 are pressurized to a low pressure, such as 45 psi (310 kPa), while the storage tanks 26, 28, 30, and 32 are high-pressure tanks capable of withstanding, for example, 1000 psi

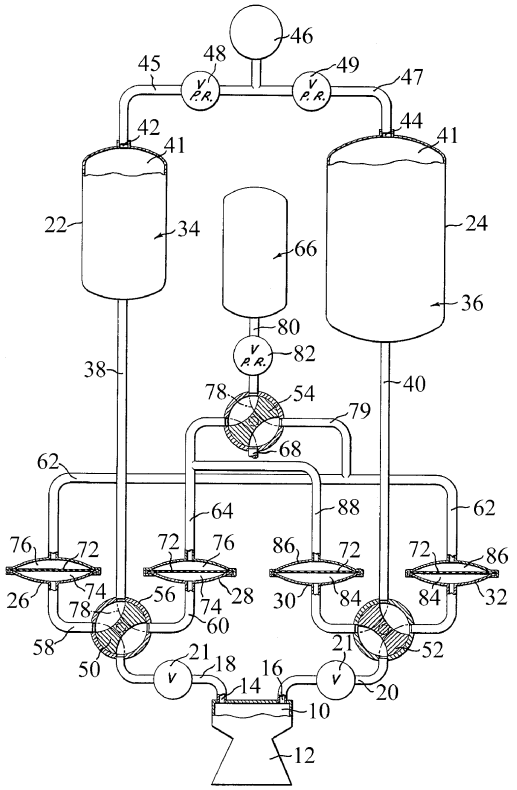

Fig. 1 Sobey pressurizer system.

(6.9 MPa). The valves 50, 52, and 54 are configured so that, as they rotate, fuel storage tanks 26 and 28 are alternately filled with fuel from low-pressure fuel tank 22, pressurized by high-pressure gas 66, and drained to combustion chamber 10, and similarly oxygen storage tanks 30 and 32 are alternately filled with oxygen from low-pressure oxygen tank 24, pressurized by high-pressure gas 66, and drained to combustion chamber 10. For example, in the valve configuration shown in Fig. 1 storage tank 26 is filling with fuel under low pressure because the lower region has a fluid connection to the fuel tank 22 and the upper region has a fluid connection to an exhaust 68; in sharp contrast storage tank 28 is draining fuel to the combustion chamber 10 under high pressure because the lower region has a fluid connection to the combustion chamber 10 and the upper region has a fluid connection to the high-pressure gas source 66. After storage tank 26 is fully filled and storage tank 28 is fully drained, valves 50 and 54 subsequently rotate 90 deg to a new valve configuration. In this new valve configuration storage tank 26 will drain fuel to the combustion chamber 10 under high pressure because the lower region will have a fluid connection to the combustion chamber 10 and the upper region will have a fluid connection to the high-pressure gas source 66, and storage tank 28 will fill with fuel under low pressure because the lower region will have a fluid connection to the fuel tank 22 and the upper region will have a fluid connection to the exhaust 68. This process is mirrored on the oxygen side with storage tanks 30 and 32 and valve 52. Because, at any given time, one of the fuel storage tanks 26 and 28 and one of the oxygen storage tanks 30 and 32 are draining at high pressure into the combustion chamber 10, the net result is an uninterrupted flow of fuel and oxidizer into the combustion chamber 10, without the need for maintaining the fuel and oxidizer tanks 22 and 24 at high pressure.

A substantially identical design was patented[3] in November 2001 by Mark Eric Lanning and James B. Blackmon, Jr., the main differences being 1) addition of a third storage tank, 2) replacement of Sobey's mechanically actuated rotating valves with independently actuated valves that allow for an overlap in the draining cycles of at least two storage tanks, and 3) addition of a feedback and control system.

Another substantially identical design was described[4] by Steve Harrington, the main differences being: 1) the use of two storage tanks, one having $\frac{1}{4}$ the volume of the other; and 2) the use of check valves between the storage tanks and the combustion chamber.

An important problem arises with the Sobey/Lanning/Harrington systems. The greatest weight savings are achieved by minimizing the size of the storage tanks because they are high-pressure vessels. However, the smaller the storage tanks are, the faster their corresponding valves must open and close; a valving rate of more than 60 cycles per second might be needed to make the Sobey/Lanning/Harrington systems competitive with current turbopump technology. Unfortunately, precision, high-speed, high-pressure, preferably cryogenic valves are both expensive and prohibitively heavy. Further, as the valving rate of the valves increases, their friction power dissipation increases. This additional friction power must ultimately be supplied by additional propellants, thus adding mass m_{friction} to the rocket.

B. Design Analysis of Prior Technology

The problem of super-high-speed valves can be illustrated by the following design analysis. A simple two-storage-tank version of the Lanning pump will be designed to substantially match the performance of the turbopump of the F-1 engine, the largest rocket engine ever built and the workhorse of the Saturn V rocket. In other words, a "plug-and-play" version of the Lanning pump will be designed such that the F-1 turbopump could be replaced with the Lanning pump without any change in performance; the mass, cost, and reliability of the two will then be compared.

The F-1 engine generated 1,522,000 lb (6,770,000 N) of thrust at sea level with a chamber pressure of 1125 psia (7.73 MPa) and a sea-level specific impulse of 265 s. The F-1 turbopump, weighing 3000 lb (1360 kg), pumped 25,000 gallons per minute of liquid oxygen (LOX) (1800 kg/s at $\rho_{\text{LOX}} = 1142$ kg/m^3) at a pressure of 1600 psia (11.0 MPa) and 15,600 gallons per minute of RP-1 (800 kg/s at $\rho_{\text{RP}-1} = 810$ kg/m^3) at a pressure of 1870 psia (12.8 MPa). The gas generator burned about 3% of the propellants, producing fuel-rich gas at 1500°F (1090 K) (Ref. 5). The molecular mass of the combustion gas from the gas generator was about 14 kg/kmol, and its isentropic parameter γ was about 1.35 (Ref. 6). As utilized in the Saturn V rocket, each F-1 engine burned a propellant mass m_{prop} of 416,000 kg in an average burn time of 160 s and lifted its $\frac{1}{5}$ portion of the Saturn V rocket to 5118 m/s (Ref. 7). At an oxidizer-to-fuel ratio of 2.25, for each F-1 engine $m_{\text{LOX}} = 290{,}000$ kg, $V_{\text{LOX}} = 254$ m^3, $m_{\text{RP}-1} = 128{,}000$ kg, and $V_{\text{RP}-1} = 158$ m^3. Liquid oxygen flowed at 37.5 m/s through an area of 424 cm^2, and RP-1 flowed at 17.5 m/s through an area of 562 cm^2.

The mass benefit that accompanies using small high-pressure propellant storage tanks (such as in Lanning's device) instead of pressurizing the entire propellant tank (such as in a conventional blowdown system) comes at a price of additional mass because more pressurant is needed to continuously stop and start the flow of propellant into and out of the storage tanks. This additional mass Δm_{pump} is calculated as follows. In any rocket-engine system the flow velocity of propellants to the combustion chamber depends on the required mass flow rate, the density ρ_{prop} of the propellant, and the cross-sectional area A_c of the conduit through which the propellant flows:

$$v = \dot{m}/\rho_{\text{prop}} A_c \tag{3}$$

Further, the timed dynamic pressure of a moving propellant can be expressed as

$$\Delta P_{\text{dynamic}}(t) = \tfrac{1}{2}\rho_{\text{prop}} v(t)^2 \tag{4}$$

Given a column of fluid sandwiched between a pressure drop $P_1 - P_2$ (as shown in Fig. 2), the total timed pressure drop $\Delta P(t)$ available to accelerate the fluid is given by

$$\Delta P(t) = P_1 - P_2 - \Delta P_{\text{dynamic}}(t) = P_1 - P_2 - \tfrac{1}{2}\rho_{\text{prop}} v(t)^2 \tag{5}$$

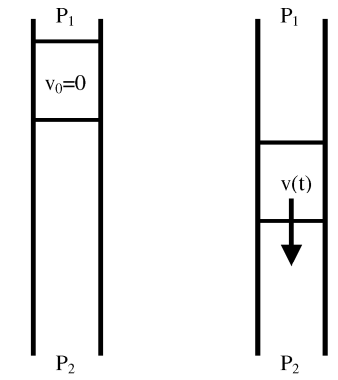

Fig. 2 Acceleration of a column of fluid.

If the column of fluid has cross-sectional area A_c and mass m, then the timed acceleration $a(t)$ on the column of fluid can be expressed as:

$$a(t) = \frac{\mathrm{d}\,v(t)}{\mathrm{d}\,t} = \frac{F(t)}{m} = \frac{\Delta P(t) A_c}{m}$$

$$= \frac{A_c}{m}\left[P_1 - P_2 - \frac{1}{2}\rho_{\text{prop}} v(t)^2\right] \tag{6}$$

Solving for $v(t)$,

$$v(t) = \sqrt{\frac{2(P_1 - P_2)}{\rho_{\text{prop}}}}\tanh\left[\frac{A_c t}{m}\sqrt{\frac{\rho_{\text{prop}}(P_1 - P_2)}{2}}\right] \tag{7}$$

The average drain velocity of the fluid, which is known for a given rocket-engine application and is determined from Eq. (3), over a drain time t_d is

$$\bar{v}_d = \frac{\int_0^{t_d} v(t)\mathrm{d}\,t}{t_d}$$

$$= \frac{2m}{A_c \rho_{\text{prop}} t_d}\,\ell_n\left\{\cosh\left[\frac{A_c t_d}{m}\sqrt{\frac{\rho_{\text{prop}}(P_1 - P_2)}{2}}\right]\right\} \tag{8}$$

Thus, the pressure drop $P_1 - P_2$ required to give the column of fluid the required average drain velocity in drain time t_d is

$$P_1 - P_2 = \frac{2m^2}{\rho_{\text{prop}} A_c^2 t_d^2}\left\{\cosh^{-1}\left[\exp\left(\frac{\bar{v}_d A_c \rho_{\text{prop}} t_d}{2m}\right)\right]\right\}^2 \tag{9}$$

Note that

$$\lim_{t_d \to \infty}(P_1 - P_2) = \frac{1}{2}\rho_{\text{prop}}\bar{v}_d^2 = \Delta P_{\text{dynamic}}(\bar{v}_d) \tag{10}$$

This implies that where t_d is sufficiently large, such as in a conventional blowdown rocket-engine system or a turbopump rocket-engine system, $P_1 - P_2$ is just the dynamic pressure of the propellant flowing at the required average drain velocity. However, in Lanning's pump, in which propellant is continuously flowing in and out of small propellant storage tanks (thus rapidly changing the propellant's momentum), t_d is sufficiently small such that $P_1 - P_2$ is substantially greater than the dynamic pressure of the propellant flowing at the required average drain velocity. P_1, corresponding to the pressure of the pressurant, must therefore be higher than a corresponding blowdown or turbopump system, and this pressure "cost" ΔP_{pres} can be calculated as

$$\Delta P_{\text{pres}} = P_1 - P_2 - \frac{1}{2}\rho_{\text{prop}}\bar{v}_d^2$$

$$= \frac{2m^2\bar{v}_d^2}{\rho_{\text{prop}} A_c^2 L^2}\left\{\cosh^{-1}\left[\exp\left(\frac{\rho_{\text{prop}} A_c L}{2m}\right)\right]\right\}^2 - \frac{1}{2}\rho_{\text{prop}}\bar{v}_d^2 \tag{11}$$

where L is the distance traveled by the column of fluid in the drain time t_d. Note that $m = \rho_{\text{prop}} A_c L$ only where the mass m consists only of propellant. In more advanced designs—which will be discussed later—the mass m can also include a piston or other barrier between the pressurant and propellant. Next, the pressurant mass cost Δm_{pres} of Lanning's pump, where V_{prop} is the total volume of the propellant, M_{pres} is the molecular mass of the pressurant, and the pressurant remains at a constant temperature T_{pres}, is given by the Ideal Gas Law:

$$\Delta m_{\text{pres}} = \frac{\Delta P_{\text{pres}} V_{\text{prop}} M_{\text{pres}}}{R_U T_{\text{pres}}} \tag{12}$$

To determine the total mass effect that ΔP_{pres} has on the mass of Lanning's pump, both of the following effects must be considered: 1) the mass $m_{\text{tank,pres}}$ of the pressurant tank increases with the mass m_{pres} of the pressurant; and 2) for a booster-class engine, because the pressurant mass decays during the engine burn, the initial pressurant mass m_{pres} is equivalent to a fixed (i.e., nondecaying) pressurant mass $m_{\text{pres,fixed}}$ that is less than the initial pressurant mass. For effect 1), a tank mass multiplier f_t is defined such that

$$f_t = \frac{\mathrm{d}(m_{\text{tank,pres}})}{\mathrm{d}(m_{\text{pres}})} \tag{13}$$

For a system utilizing a gas generator system, f_t is negligible because the pressurant initially exists as low-pressure liquid propellant; however, for a system utilizing a pressurant tank containing high-pressure helium at 300 K, f_t is typically greater than 20. In other words, adding 1 kg of pressurant to a rocket-engine system employing a gas generator will add very little (i.e., $\ll$1 kg) to its tanks, but will add 20 kg or more to the pressurant tank of a rocket employing a high-pressure helium pressurant tank. For effect 2), a pressurant mass equivalence factor f_e is defined such that

$$f_e = \frac{\mathrm{d}(m_{\text{pres,fixed}})}{\mathrm{d}(m_{\text{pres}})} \tag{14}$$

For an in-space control system $f_e \approx 1$, whereas for a booster rocket-engine system, f_e can be determined by the following. First, the final (postburn) mass m_f of a rocket depends on the total mass m_{prop} of propellant, the change in velocity Δv caused by the engine burn, and the specific impulse I_{sp} of the engine[8]:

$$m_f = m_{\text{prop}}[\exp(\Delta v / g_0 I_{\text{sp}}) - 1]^{-1} \tag{15}$$

If a small additional mass Δm_{pres} of pressurant is treated as additional propellant, then the final mass m_f of the rocket remains unchanged, but the propellant mass increases to $m^*_{\text{prop}} = m_{\text{prop}} + \Delta m_{\text{pres}}$, and the specific impulse decreases to I^*_{sp}:

$$I^*_{\text{sp}} = I_{\text{sp}}\left(\frac{m_{\text{prop}}}{m_{\text{prop}} + \Delta m_{\text{pres}}}\right) \tag{16}$$

If, instead, the additional mass Δm_{pres} of pressurant is treated as a small additional fixed mass $\Delta m_{\text{pres,fixed}}$, then the propellant mass m_{prop} and specific impulse I_{sp} remain unchanged, but the final mass increases to $m^*_f = m_f + \Delta m_{\text{pres,fixed}}$. Solving for $\Delta m_{\text{pres,fixed}}$,

$$\Delta m_{\text{pres,fixed}} = m_{\text{prop}}\Big/\left[\exp\left(\frac{\Delta v}{g_0 I_{\text{sp}}}\right) - 1\right]$$

$$- m^*_{\text{prop}}\Big/\left[\exp\left(\frac{\Delta v}{g_0 I^*_{\text{sp}}}\right) - 1\right] \tag{17}$$

The pressurant mass equivalence factor f_e can now be determined by substituting Eq. (17) into Eq. (14). For the Saturn V rocket, $f_e = 20.7\%$. In other words, adding 1 kg of pressurant (in the form of propellant) to this rocket-engine system would be equivalent to adding only 0.207 kg of dead weight to the system. Thus, the total mass effect Δm_{pump} that ΔP_{pres} has on the mass of Lanning's pump is

$$\Delta m_{\text{pump}} = (f_t + f_e)\Delta m_{\text{pres}} \tag{18}$$

The total mass of the Lanning LOX pump includes several portions. Besides Δm_{pump} and the mass m_{tank} of each of two storage tanks, the Lanning LOX pump also includes the following:

1) The mass m_{acc} of a propellant accumulator is included. According to Eq. (7), $v(t)$ varies with time, causing pulsations in the propellant flow rate. To ensure a constant flow rate, a propellant accumulator must be added.

2) The mass m_{piston} of each of two pistons, diaphragms, or other separators between the pressurant and propellant (i.e., one piston for each storage tank) is also included. The piston/separator serves the following functions: a) to reduce heat transfer from the pressurant to the propellant; b) to prevent pressurant from being injected into the combustion chamber and to prevent propellant from being exhausted from the pump; c) to prevent chemical reaction between the pressurant and propellant; and d) to prevent sloshing of the propellant. Function a) is particularly important where the pressurant is hot gas from a gas generator and the propellant is cryogenic. If the piston is a differential piston (i.e., the two ends have different cross sectional areas), the piston can serve a fifth function: e) to eliminate the need for an additional gas generator pump (i.e., a pump that pumps propellants into the gas generator). Function e) requires that the volume and corresponding mass m_{tank} of each tank are more than twice what they would otherwise be.

3) The mass m_{valves} of the valves is also included.

4) The mass m_{friction} of the additional propellants burned in friction power dissipation of the valves is included.

5) The mass m_{ggpump} of a gas generator pump is also included. As shown in Eq. (9), the pressure P_1 of gas generated by the gas generator is substantially greater than the pressure P_2 of propellant flowing from the pump exit. To provide a constant flow of propellant to the gas generator, a gas generator pump is needed to pump propellant from pressure P_2 to the gas generator injection pressure $P_{\text{gg}} = P_1 + \Delta P_{\text{inj}}$. A gas generator pump can be avoided by using differential pistons in the storage tanks, as just discussed, but with the detriment of heavier storage tanks. Clearly, in a system using a high-pressure gas pressurant tank (e.g., helium) instead of a gas generator there is no need for a gas generator pump.

Therefore, the total mass of the Lanning LOX pump can be expressed as

$$m_{\text{LOXpump}} = \Delta m_{\text{pump}} + 2m_{\text{tank}} + m_{\text{acc}} + 2m_{\text{piston}} + m_{\text{valves}} + m_{\text{friction}} + m_{\text{ggpump}} \tag{19}$$

Next, the mass m_{tank} of each tank will be approximated. Although a sphere yields the lowest mass/volume ratio for a high-pressure storage tank, a sphere is an impractical shape for the Lanning pump design. Thus, a spherical cylinder—a cylinder having radius r and length $L = 4r/3$, such that its volume of $(4/3)\pi r^3$ is the same as the volume of a sphere having radius r—will be used. It will be assumed that the mass of a spherical cylinder tank is twice the mass of a spherical tank having the same volume [from Eq. (1)]. Thus,

$$m_{\text{tank,cylinder}} = \frac{2P_b V_{\text{tank}}}{\phi_{\text{tank}} g_0} \tag{20}$$

The mass m_{tank} is a bare-bones approximation that does not include the additional volume required for a piston, diaphragm, or other separator between the pressurant and propellant.

The mass m_{acc} of the accumulator can be calculated by recognizing that it will need to supply the difference between the average drain velocity and the actual drain velocity $v_d(t)$ from the beginning of the drain cycle until the flow has reached the average drain velocity:

$$m_{\text{acc}} = \left(\frac{V_{\text{acc}}}{V_{\text{tank}}}\right) m_{\text{tank}} = \frac{A\int_0^{t(\bar{v}_d)} [\bar{v}_d - v_d(t)]\,\mathrm{d}t}{AL} m_{\text{tank}} = \frac{m_{\text{tank}}}{L}\int_0^{t(\bar{v}_d)} [\bar{v}_d - v_d(t)]\,\mathrm{d}t \tag{21}$$

For t_d very small, $m_{\text{acc}} \approx \frac{1}{4} m_{\text{tank}}$.

The mass m_{valves} of the valves is particularly difficult to approximate because it will depend on many factors, such as the type of valve, fluid flow area, pressure differential, and, most importantly, reaction time t_{reaction} (i.e., the time required to fully open and close). Steve Harrington suggests that the mass m_{valves} of a system having a cycle time t_{cycle} of 5 s is 25% the mass of the two storage tanks.[4] As t_{cycle} decreases, however, t_{reaction} must also decrease, and the moving valve parts must accelerate more quickly, requiring larger forces, and, ultimately, heavier parts. For example, to decrease t_{reaction} of an electric valve having a solenoid and a valve plate will require a larger, heavier solenoid to accelerate the valve plate more quickly. Thus, m_{valves} will not be solved explicitly here. Similarly, m_{piston}, m_{friction}, and m_{ggpump} will not be solved explicitly here.

For simplicity of calculation, the following assumptions about the Lanning pump design will be made: 1) the storage tanks do not have pistons/separators, so that $m = \rho_{\text{prop}} A_c L$ in Eq. (11); and 2) the pressurant is hot gas from a gas generator, so that $f_t \approx 0$. Although these assumptions will yield a minimum mass, they are, in fact, incompatible. A system utilizing a gas generator must have pistons/separators to separate the hot pressurant from the cryogenic propellant, so that $m > \rho_{\text{prop}} A_c L$ and Δm_{pres} [from Eqs. (11) and 12)] increases. Conversely, a system without pistons/separators must use a high-pressure pressurant tank, so that $f_t \gg 1$ and Δm_{pump} [from Eq. (18)] increases. Therefore, an actual rocket-engine system utilizing a Lanning pump will be substantially heavier than the following calculations suggest.

Because the drain time t_d is about half the cycle time t_{cycle} for a system having two storage tanks and because the volume V_{tank} of the storage tank and the average drain velocity can each be expressed in terms of the cycle time t_{cycle}, as shown next, the total mass m_{LOXpump} of the Lanning LOX pump can also be expressed in terms of the cycle time t_{cycle} [by substituting Eqs. (11–14), (18), (20), and (21) into Eq. (19)]:

$$V_{\text{tank}} = \frac{\dot{m} t_{\text{cycle}}}{2\rho_{\text{prop}}} = \frac{4}{3}\pi r^3 \tag{22}$$

$$\bar{v}_d = \frac{2L}{t_{\text{cycle}}} = \frac{2\left(\frac{4}{3}r\right)}{t_{\text{cycle}}} = \sqrt[3]{\frac{64\dot{m}}{9\pi\rho_{\text{prop}} t_{\text{cycle}}^2}} \tag{23}$$

$$m_{\text{LOXpump}} = \left[(f_t + f_e)\left(\frac{V_{\text{prop}} M_{\text{pres}} \rho_{\text{prop}}^{\frac{1}{3}} \dot{m}^{\frac{2}{3}}}{R_U T_{\text{pres}}}\right)\left(\frac{64}{9\pi}\right)^{\frac{2}{3}} \times \left(2\left\{\cosh^{-1}\sqrt{e}\right\}^2 - \frac{1}{2}\right)\right] t_{\text{cycle}}^{-\frac{4}{3}} + \left(\frac{2.25 P_b \dot{m}}{\phi_{\text{tank}} g_0 \rho_{\text{prop}}}\right) t_{\text{cycle}} + m_{\text{valves}} + m_{\text{friction}} + m_{\text{ggpump}} \tag{24}$$

Using parameters of the F-1 engine and Saturn V rocket given earlier, choosing $\phi_{\text{tank}} = 2500$ m, and letting

$$m_{\text{LOXpump}} = \left(0.401 t_{\text{cycle}}^{-\frac{4}{3}} + 3180 t_{\text{cycle}} + m_{\text{valves}} + m_{\text{friction}} + m_{\text{ggpump}}\right) \text{kg} \tag{25}$$

Notice that the Δm_{pump} term (the first term) is significant only where t_{cycle} is substantially less than a second. A large tank mass factor ϕ_{tank} (corresponding to a structurally simple, basic tank consisting of fiber-reinforced composite materials) is not appropriate here. The tank mass factor ϕ_{tank} is chosen as 2500 m for at least two reasons: 1) because of the presence of large, heavy, fast-acting valves, a significant portion of each tank consists of connections/welds to these valves, as well as the additional structure necessary to support the weight and vibrations of these valves; and 2) the fast acceleration and deceleration of the propellant column inside the storage tank causes a water hammer effect (and its resulting high-pressure fluctuations) against which the tank must be designed.

The minimum feasible cycle time t_{cycle} for the system can be estimated as follows. One complete cycle consists of the following 11 events: 1) opening of pressurant entrance valve in $t_{\text{valve,pres}}$;

2) opening of propellant drain valve in $t_{\text{valve,drain}}$; 3) draining of propellant in t_d; 4) closing of propellant drain valve in $t_{\text{valve,drain}}$; 5) closing of pressurant entrance valve in $t_{\text{valve,pres}}$; 6) opening of pressurant vent valve in $t_{\text{valve,vent}}$; 7) venting of pressurant in t_{vent}; 8) opening of propellant entrance valve in $t_{\text{valve,fill}}$; 9) filling of propellant in t_f; 10) closing of propellant entrance valve in $t_{\text{valve,fill}}$; and 11) closing of pressurant vent valve in $t_{\text{valve,vent}}$. Further, 1) and 2) must occur before 3); 3) must occur before 4) and 5); 4) and 5) must occur before 6) and 7); 6) and 7) must occur before 8) and 9); 8) and 9) must occur before 10) and 11); and 10) and 11) must occur before 1) and 2) of the next cycle. Assuming that each of the valving operations has the same valving time t_{valve}, then the cycle time t_{cycle} is limited by

$$t_{\text{cycle}} > t_d + 5t_{\text{valve}} = 10t_{\text{valve}} \tag{26}$$

In the actual F-1 engine the main LOX valves open in $\frac{1}{3}$ s, the main fuel valves open in $\frac{2}{3}$ s, and the gas generator valves open in 170 ms and close in 90 ms (Ref. 5). Assuming that $t_{\text{valve}} = 100$ ms for typical valves of this magnitude, $t_{\text{cycle}} > 1$ s. This calculation is consistent with Lanning's suggested cycle time t_{cycle} of 6 s (Ref. 3) and Harrington's suggestion that $t_{\text{cycle}} = 5$ s but can be driven as low as 1 s (Ref. 4).

For $t_{\text{cycle}} = 1$ s, Eq. (25) yields $m_{\text{LOXpump}} > 3180$ kg. A similar analysis for the RP-1 pump yields a mass $m_{\text{fuelpump}} > 2320$ kg. Thus, the total mass of a Lanning pump system to match the performance of the F-1's 1360-kg turbopump is greater than 5500 kg.

The mass of each pump can be reduced by reducing its t_{cycle}—but only to a certain lower limit. The optimum cycle time t_{optimum}—that is, the cycle time t_{cycle} corresponding to the minimum mass of each pump—can be calculated by setting

$$\frac{\mathrm{d}m_{\text{pump}}(t_{\text{optimum}})}{\mathrm{d}t_{\text{cycle}}} = 0 \tag{27}$$

Neglecting m_{valves}, m_{friction}, and m_{ggpump} in Eq. (25) for the calculation of the optimum cycle time, $t_{\text{optimum}} = 24.1$ ms for the LOX pump and $t_{\text{optimum}} = 17.0$ ms for the RP-1 pump. Although conventional Sobey/Lanning/Harrington systems are incapable of attaining such rapid cycle times, any technology so capable holds promise for the accompanying substantial mass savings.

III. New Pressurizer

A. Description of the New Pressurizer

In December 2002 the author received a patent[9] on a pressurizer for a rocket engine that solves the problems imposed by the Sobey/Lanning/Harrington systems. The invention succeeds by utilizing the connection of three distinct, simple, unitary parts as a low-friction, ultrafast valving mechanism for an unlimited number of tiny storage tanks.[10] Thus, instead of a plethora of heavy, expensive valves that become heavier, more expensive, and less reliable with shorter cycle time, the invention uses three simple parts—only one of which moves—having a weight, cost, and reliability that are insensitive to the choice of cycle time, to provide a cycle time t_{cycle} as short as necessary. Further, the present invention is self-regulating, thus eliminating the need for a complicated sensor, feedback, and control system. The three simple parts of the pressurizer according to the present invention will be described with reference to Figs. 3–6.

The pressurizer, for a monopropellant or hybrid rocket engine system (i.e., one liquid propellant), is intended to replace storage tanks 26, 28 and rotating valves 50, 54 of Sobey. For a bipropellant system two such pressurizers can be used, the second pressurizer intended to replace storage tanks 30, 32 and rotating valve 52 of Sobey. The pressurizer comprises a top chamber separator, a bottom chamber separator, and a spindle, as shown in Figs. 3–5. The top chamber separator has two holes: the first is a high-pressure pressurant entrance that is connected via conduit to the pressurant tank (e.g., high-pressure helium) or the gas generator; the second is an exhaust or vent to ambient pressure. The bottom chamber separator also has two holes: the first, which is lined up with the pressurant entrance of the top chamber separator, is a propellant exit that is connected via conduit to the rocket-engine combustion chamber; the second, which is lined up with the exhaust hole of the top chamber separator, is a propellant entrance that is connected via conduit to the propellant tank. The spindle is a cylinder having a large number of preferably cylindrical holes running through its length, where each hole acts as an individual storage tank (or, more descriptively, a transfer chamber); the volume of each transfer chamber is substantially smaller than that of Sobey's storage tanks 26, 28, 30, 32. The spindle is located between the top and bottom

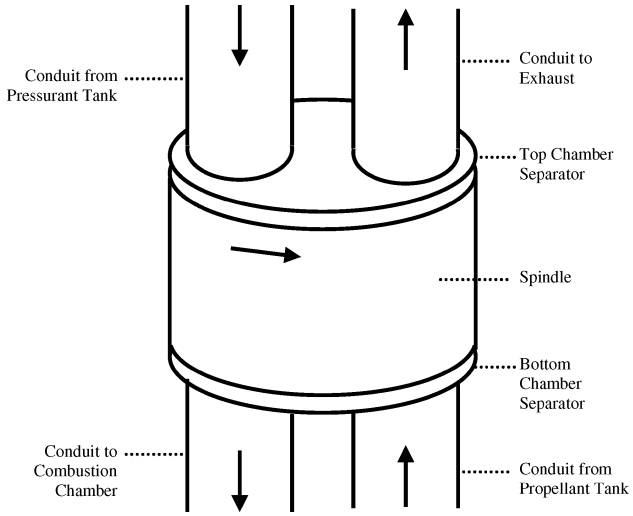

Fig. 3 Perspective view of the pressurizer.

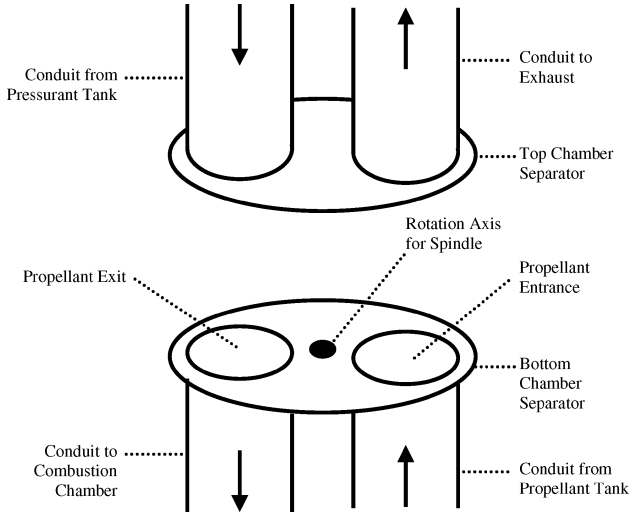

Fig. 4 Perspective view of the pressurizer without the rotatable spindle.

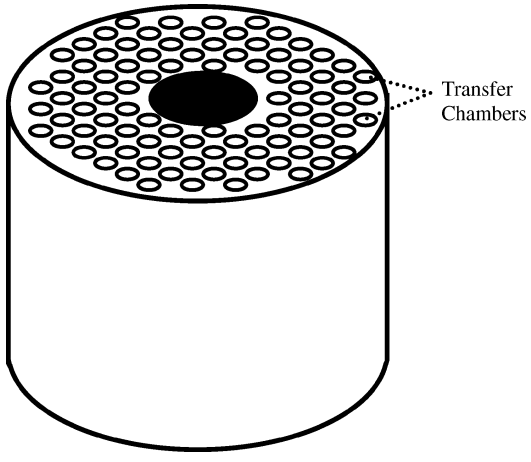

Fig. 5 Perspective view of the spindle.

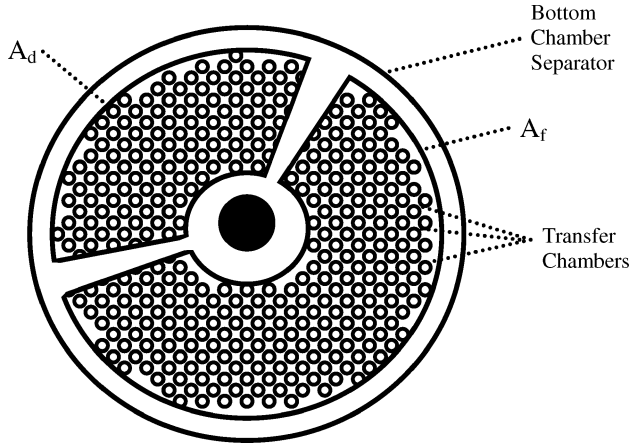

Fig. 6 Bottom view of bottom chamber separator, showing spindle through propellant entrance and exit holes.

chamber separators so that it can rotate with respect to the chamber separators and so that there is a reasonably good seal between the top chamber separator, the spindle, and the bottom chamber separator. By convention, the region located between the exhaust hole of the top chamber separator and the propellant entrance of the bottom chamber separator is the "filling region"; the region located between the pressurant entrance of the top chamber separator and the propellant exit of the bottom chamber separator is the "draining region." The chamber separators have the purpose of separating (i.e., preventing a fluid connection between) transfer chambers in the filling region and transfer chambers in the draining region.

Figure 6 shows a bottom view of a bottom chamber separator according to a preferred embodiment of the present invention; the spindle (and its transfer chambers) can be seen through the holes of the bottom chamber separator. In this embodiment the bottom chamber separator has a propellant entrance hole (corresponding to the filling region) having an area A_f (bounded by a radial width α_f) and a propellant exit hole (corresponding to the draining region) having an area A_d (bounded by a radial width α_d), and the spindle comprises hundreds of small cylindrical transfer chambers that are small enough so that many of them are located in the draining region at any given time.

In operation, the spindle rotates, causing the pressurizer to transfer propellant from the propellant tank at low pressure to the combustion chamber at high pressure in a continuous flow upon the force of the high-pressure pressurant. The operation can be described by considering a single transfer chamber as the spindle moves through one full rotation. Because the holes in the chamber separators have fixed radial widths α_f and α_d, it takes a fill time $t_f = \alpha_f/(r_r \times 360 \text{ deg})$ for a transfer chamber to fully traverse the filling region after it has entered the filling region and a drain time $t_d = \alpha_d/(r_r \times 360 \text{ deg})$ for a transfer chamber to fully traverse the draining region after it has entered the draining region, where r_r is the spindle rotation rate. At first, the empty transfer chamber is located at the beginning of the filling region—that is, it has just entered the filling region. Because any high-pressure pressurant inside the transfer chamber quickly vents via the exhaust hole, the pressure inside the transfer chamber quickly drops to a pressure lower than that inside the propellant tank, and propellant fills up inside the transfer chamber. As the spindle rotates, the transfer chamber fills with propellant as it traverses the filling region. If the rotation rate r_r of the spindle is optimized, the transfer chamber will completely fill in the fill time t_f. As the spindle continues to rotate, the transfer chamber exits the filling region and enters the draining region, where the pressurant enters the transfer chamber via the pressurant entrance hole in the top chamber separator and exerts a force on the propellant inside the transfer chamber, thus pushing the propellant into the combustion chamber via the propellant exit hole in the bottom chamber separator. Again, if the rotation rate r_r is optimized, the transfer chamber will completely drain in the drain time t_d. As the spindle continues to rotate, the transfer chamber exits the draining region and again enters the filling region, where the cycle begins again. Because the spindle has many transfer chambers, always at least one transfer chamber is draining propellant to the combustion chamber under the force of the pressurant. Therefore, the pressurizer according to this invention provides a constant flow of high-pressure propellant without the need for a turbopump, thick-walled propellant tanks, or a complicated network of valves. Further, because the rotation rate r_r can be chosen arbitrarily high, a very low cycle time t_{cycle}, with the accompanying low pump mass, can be obtained.

A further benefit of this pressurizer is that the ratio t_f/t_d can be selected (by varying the radial widths α_f and α_d of the filling and draining regions, respectively) such that the time available for each transfer chamber to fill is greater than the time available to drain; this allows for a corresponding pressure drop ratio between the filling and draining regions. This is a desirable feature because the pressure drop across the filling region is limited by the pressure in the propellant tank, which is typically 45–75 psia (310–520 kPa). In other words, the propellant mass flow rate from the propellant tank to the pressurizer can be equated to the propellant mass flow rate from the pressurizer to the combustion chamber, even where the pressure drop across the filling region is less than that of the draining region, by setting

$$t_f/t_d = \alpha_f/\alpha_d = \sqrt{\Delta P_d/\Delta P_f} \tag{28}$$

A problem with the preceding free-flow design is that the meniscus of the propellant inside each transfer chamber can move freely, that is, there is nothing to prevent the propellant meniscus from moving outside of the transfer chamber. Such a design requires that the rotation rate r_r of the spindle, as well as the ratio of pressure differentials $\Delta P_d/\Delta P_f$ in the draining and filling regions, must be chosen and sustained perfectly, such as with a complicated sensor/control system. Otherwise, if the rotation rate r_r is too slow propellant will be ejected from the exhaust hole as each transfer chamber is overfilled in the filling region, and pressurant will be injected into the combustion chamber as each transfer chamber is overdrained in the draining region. If the rotation rate r_r is too fast and if the ratio of pressure differentials $\Delta P_d/\Delta P_f$ in the draining and filling regions is not perfectly correlated to the ratio t_f/t_d, as in Eq. (28), the propellant meniscus in each transfer chamber will, over time, migrate upwards or downwards, until either propellant is ejected from the exhaust hole or pressurant is injected into the combustion chamber. These problems—and their need for a complicated sensor/control system—can be avoided by equipping each transfer chamber with a movable separator, such as a piston or membrane, configured to separate the propellant and pressurant and to prevent ejection of propellant from the exhaust hole or pressurant into the combustion chamber.

Figures 7a–7c show cross sections of four adjacent transfer chambers in the draining region under three different conditions (as shown), each assuming a constant spindle rotation rate r_r. The separator inside each transfer chamber is a bearing ball whose movement is limited at each end of the transfer chamber. Figure 7c shows how the existence of the separator (e.g., bearing ball) prevents leakage of pressurant into the combustion chamber, but also requires that multiple transfer chambers are located in the draining region at any given time to ensure a continuous propellant flow into the combustion chamber. Thus, the design depicted in Fig. 6 provides an uninterrupted flow of propellant into the combustion chamber without the necessity of perfectly satisfying $\Delta P_d = \Delta P_f(\alpha_f/\alpha_d)^2$ for every possible rotation rate r_r.

B. Design Analysis of the New Pressurizer

The benefits of the present invention will be illustrated by the following design analysis. As in the preceding design analysis of a Lanning pump, a plug-and-play version of the new pressurizer/pump will be designed to substantially match the performance of the F-1 engine, the characteristics of which were described earlier.

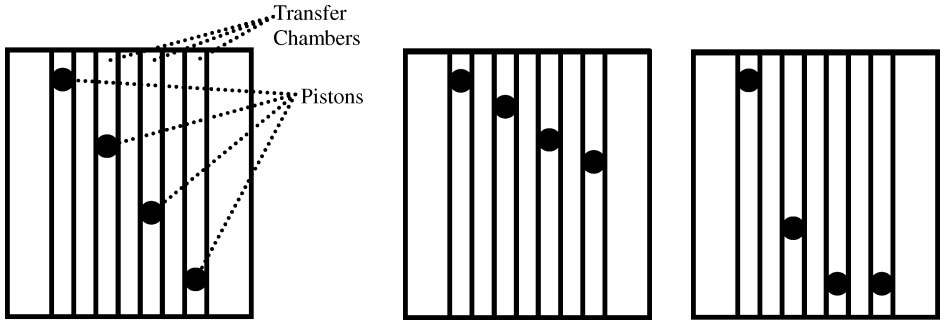

Fig. 7 Cross-sectional view of pistons in transfer chambers.

The total mass of a new LOX pump according to the present invention differs from the total mass of the Lanning LOX pump, as in Eq. (19), in the following ways:

1) Because the mass m_{acc} of the accumulator is limited to $\frac{1}{4}$ the mass m_{tank} of one storage tank, as in Eq. (21), the accumulator mass m_{acc} becomes insignificant as the number of storage tanks increases. In fact, where the new LOX pump contains several hundred transfer chambers (as it will), the fluctuations in the propellant mass flow caused by transfer chambers reaching the end of the draining cycle are so small that no accumulator is needed at all.

2) Unlike a typical contact valve, in which the friction power dissipation is substantial, rotation of the spindle of the present invention requires very little energy. Pressurant and propellant leakage from between the spindle and top and bottom chamber separators (discussed and quantified later) act as a fluid bearing, thus minimizing frictional losses caused by spindle rotation. The spindle can be easily rotated with the energy available in the exhausted high-pressure pressurant, so that no additional propellant mass m_{friction} is required to provide this friction power dissipation.

3) The new LOX pump, unlike the Lanning pump, leaks pressurant from between the spindle and the top chamber separator and propellant from between the spindle and the bottom chamber separator. However, by containing the new LOX pump inside a leakage shroud to catch the leaked propellant and including a small electric or pneumatic leakage pump to pump the leaked propellant from ambient pressure to the propellant tank pressure [merely 45–75 psia (310–520 kPa)], the leakage consists of pressurant mass Δm_{direct} directly leaked (i.e., directly from between the spindle and the top chamber separator) and pressurant mass $\Delta m_{\text{indirect}}$ indirectly leaked (i.e., the pressurant needed to repump the salvaged propellant), as quantified next. As in Eq. (18), the total mass effect $\Delta m_{\text{leakage}}$ that leakage has on the mass of the new pump is adjusted by the values of f_t and f_e.

The masses $2m_{\text{tank}}$, $2m_{\text{piston}}$, and m_{valves} in Eq. (19) are replaced by a single term m_{pump}, where the mass of the pump m_{pump} includes the mass m_{spindle} of the spindle and the masses of the top and bottom chamber separators (having appropriate plumbing), an axle and bearing on which the spindle spins, the pistons/diaphragms in the transfer chambers, the electric or pneumatic motor to spin the spindle, the leakage shroud and pump, and the structure to hold the spindle and chamber separators together (as they are being pulled apart by the pressure of the pressurant). The design and construction of a working prototype of the present invention (as discussed later) indicate that $m_{\text{pump}} \approx 3m_{\text{spindle}}$.

Thus, the total mass $m_{\text{newLOXpump}}$ of a new LOX pump according to the present invention can be expressed as:

$$m_{\text{newLOXpump}} = m_{\text{pump}} + \Delta m_{\text{pump}} + \Delta m_{\text{leakage}} + m_{\text{ggpump}}$$
$$= 3m_{\text{spindle}} + (f_t + f_e)(\Delta m_{\text{pres}} + \Delta m_{\text{direct}} + \Delta m_{\text{indirect}}) + m_{\text{ggpump}} \quad (29)$$

Because the bottom chamber separator shown in Fig. 6 is asymmetrical about the axis of spindle rotation, the difference in pressures in the filling and draining regions can cause undesirable torques on the top and bottom chamber separators. Thus, in a preferred embodiment of the present invention the top and bottom chamber separators are symmetric about the axis of spindle rotation, as shown in Fig. 8, thus providing two complete draining and filling cycles per spindle rotation. Figure 8 shows, in solid outline, the propellant entrance and propellant exit holes in the bottom chamber separator. Figure 8 shows that one 180-deg cycle in the bottom chamber separator consists of a draining region having radial width α_d, two space or separation regions each having radial width α_{space}, a filling region having radial width α_f, and a depressurization region having radial width α_{dep}. The space/separation regions must be wide enough to prevent a direct flowpath from the draining region to the filling region. The depressurization region must be wide enough to allow the high-pressure pressurant in each transfer chamber to depressurize to (or below) the propellant tank pressure before the transfer chamber is aligned with the propellant entrance hole, otherwise, propellant backflow can occur. The pressurant entrance and exhaust holes in the top chamber separator have a similar configuration to that shown in Fig. 8, except that the exhaust hole in the top chamber separator is extended by radial width α_{dep} to allow each transfer chamber to depressurize before filling with propellant in the filling region, as shown by the dashed line in Fig. 8. Each of the holes in the top and bottom chamber separators are further defined by radii r_1 and r_2, as shown.

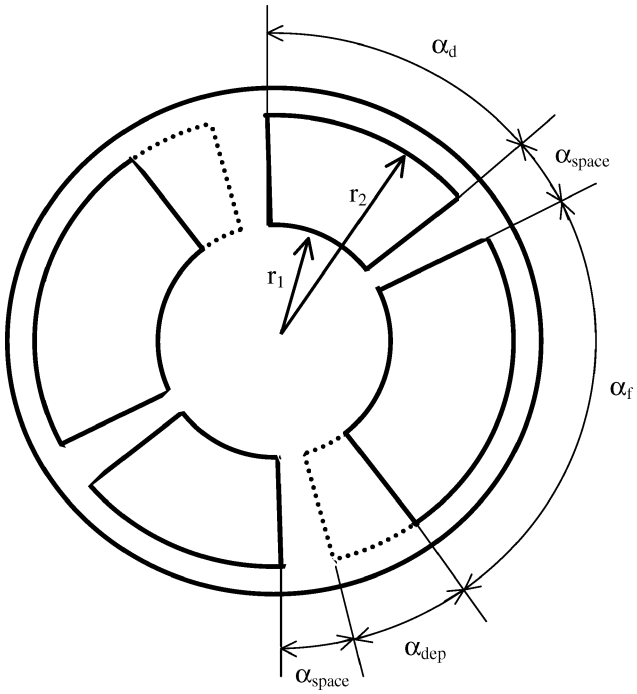

Fig. 8 Schematic view of a bottom chamber separator.

Figure 9 shows a cross-sectional view of a preferred embodiment of the spindle. (Only the basic design is depicted; in implementing the design, the diameter of the transfer chambers would be far smaller, so that the spindle contains up to several hundred transfer chambers.) Each transfer chamber comprises a lower-pressure region having a cross-sectional area A_{LP} and a higher-pressure

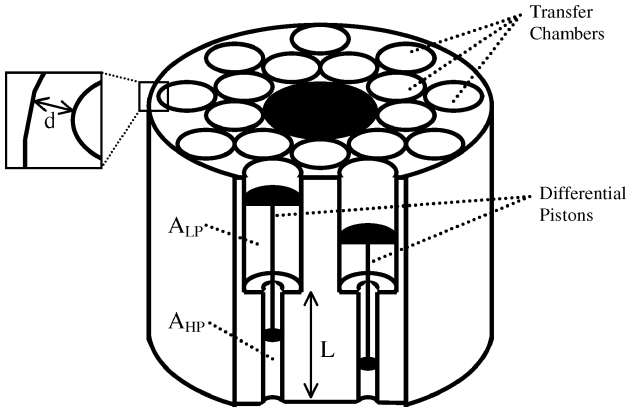

Fig. 9 Cross-sectional view of spindle having differential pistons.

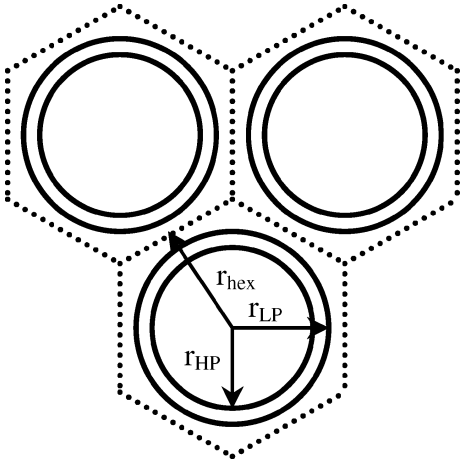

Fig. 10 Transfer chambers in regular hexagonal configuration.

region having a smaller cross-sectional area A_{HP}, each region having a length L. The regions are separated by a movable differential piston, also having a length L. Because $A_{LP} > A_{HP}$, the differential piston allows a lower-pressure fluid having pressure P_{LP} to compress a higher-pressure fluid having pressure P_{HP}, as long as $A_{LP} * P_{LP} \geq A_{HP} * P_{HP}$. Thus, by choosing A_{LP}/A_{HP} correctly the system need not include a gas generator pump and m_{ggpump} can be eliminated from Eq. (29). As a design choice, $A_{LP} = 1.2A_{HP}$ allows for a sufficient pressure drop across the gas generator's propellant injector, with a remaining pressure head sufficient to induce the required propellant mass flow rate from the pressurizer to the gas generator. In the present invention $P_{HP} = P_{outlet} + \Delta P_{pres}$ [as in Eq. (11)], where P_{outlet} is the pressure of propellant flowing from the pressurizer. For example, to match the performance of the LOX pump of the F-1 turbopump ($P_{outlet} = 11.0$ MPa) the higher pressure region of each transfer chamber must have a pressure $P_{HP} = (11.0 + \Delta P_{pres})$ MPa. Similarly, the pressure P_{LP} in each lower-pressure region (corresponding to the pressure of the pressurant gas coming from the gas generator) is reduced by the ratio of cross-sectional areas, so that $P_{LP} = P_{HP} * (A_{HP}/A_{LP})$. The piston also serves the function of thermally isolating the lower-pressure region (which can contain hot pressurant from the gas generator) from the higher-pressure region (which can contain a cryogenic propellant), thus allowing for cryogenic operation. Also shown in Fig. 9, the outer edge of the outermost transfer chamber is separated from the outer edge of the spindle by a distance d. Similarly, but not shown, the inner edge of the innermost transfer chamber is separated from the inner edge of the spindle by the distance d.

For simplicity of design, the spindle can be created by drilling holes into a cylinder. To maximize the fraction f_{LP} of lower-pressure region cross-sectional area to spindle cross-sectional area (to reduce the required spindle mass $m_{spindle}$ for a given application), the transfer chambers are located in a regular hexagonal configuration, as shown in Fig. 10. Figure 10 shows a top view of three transfer chambers in the spindle, each transfer chamber located inside an imaginary regular hexagon. Each imaginary hexagon has a radius r_{hex}, and each transfer chamber has a radius r_{LP} for the lower-pressure region and a radius r_{HP} for the higher-pressure region, as shown. Note that $A_{LP} = \pi r_{LP}^2$ and $A_{HP} = \pi r_{HP}^2$. The minimum thickness of the walls between the cylindrical transfer chambers, $2(r_{hex} - r_{LP})$, is sufficient to contain the pressure P_{LP} inside the lower-pressure region of each transfer chamber. Assuming an additional acceleration and safety margin of 2.0, this wall thickness is given by

$$2(r_{hex} - r_{LP}) = 2P_b r_{LP}/F_{all} \tag{30}$$

where P_b is the design burst pressure in the lower-pressure region (typically twice the pressure P_{LP} in the lower-pressure region). F_{all} will range from around 400 MPa for Al-2219 to 1.2 GPa for titanium.[11] Thus, using simple geometry and substituting from Eq. (30),

$$f_{LP} = \frac{\left(\pi r_{LP}^2\right)}{\left[\left(6/\sqrt{3}\right) r_{hex}^2\right]} = \frac{\pi\sqrt{3}}{6}\left(\frac{F_{all}}{F_{all} + P_b}\right)^2 \tag{31}$$

Next, the fraction f_{HP} of higher-pressure region cross-sectional area to spindle cross-sectional area is just f_{LP} reduced by the ratio A_{LP}/A_{HP}. For $A_{LP}/A_{HP} = 1.2$, $f_{HP} = f_{LP}/1.2$. So, for a propellant exit hole having a drain area A_d the total cross-sectional area through which propellant can flow from the spindle is reduced by the ratio f_{HP}, as calculated earlier and in Eq. (31). Referring to Fig. 9 and using basic geometry, the mass $m_{spindle}$ can be approximated by

$$m_{spindle} = \left(\pi r_2^2 - \pi r_1^2\right) L\rho_{spindle}(2 - f_{LP} - f_{HP}) + 4\pi(r_1 + r_2)\, d\, L\rho_{spindle} \tag{32}$$

Because d, L, $\rho_{spindle}$, and the ratio r_2/r_1 are (to some extent) design choices and because f_{LP} and f_{HP} depend primarily on the required pressure of the pressurant (e.g., gas output from the gas generator), $m_{spindle}$ can be calculated from r_1, which is determined as follows.

Modifying Eq. (3), the drain area A_d can be related to the required propellant mass flow rate for a given application by

$$\dot{m} = \rho_{prop} f_{HP} A_d \bar{v}_d \tag{33}$$

where the average drain velocity is given in Eq. (8). From Fig. 8 and using simple geometry, the total drain area A_d can be calculated. Combining this calculation with Eqs. (31) and (33) yields

$$A_d = \frac{2\alpha_d}{360\text{ deg}}\left(\pi r_2^2 - \pi r_1^2\right) = \frac{\dot{m}}{\rho_{prop}\bar{v}_d}(1.2)\left(\frac{6}{\pi\sqrt{3}}\right)\left(1 + \frac{P_b}{F_{all}}\right)^2 \tag{34}$$

Next, the radial width α_d of the draining region is chosen as a function of the drain time t_d and the rotation rate r_r of the spindle:

$$\alpha_d = t_d r_r(360\text{ deg}) = r_r L(360\text{ deg})/\bar{v}_d \tag{35}$$

Combining Eqs. (34) and (35), and choosing $r_2 = 2r_1$ (a design choice) yields r_1 as a function of $r_r L$:

$$r_1 = (1/\pi)(1 + P_b/F_{all})\left(\dot{m}/\sqrt{3}\rho_{prop} r_r L\right)^{\frac{1}{2}} \tag{36}$$

Next, the radial width α_{space} of the space/separation region is chosen such that its minimum arc length (i.e., its arc length at the inner radius r_1) is greater than twice the radius r_{LP} of the lower-pressure region of each transfer chamber by, for example, 25% (a design choice):

$$2\pi r_1(\alpha_{space}/360\text{ deg}) = 1.25(2r_{LP}) \tag{37}$$

Next, the radial width α_f of the filling region can be determined by recognizing that the pressure difference ΔP_f across the filling region available to accelerate propellant from the propellant tank into the pressurizer is limited by the pressure in the propellant tank (which is a design condition). Rewriting Eq. (11) as a function of the average fill velocity (instead of the average drain velocity) yields

$$\bar{v}_f = \frac{A_{\mathrm{HP}}L}{m}\left[\frac{(\Delta P_f)\rho_{\mathrm{prop}}}{2}\right]^{\frac{1}{2}}\left\{\cosh^{-1}\left[\exp\left(\frac{\rho_{\mathrm{prop}}A_{\mathrm{HP}}L}{2m}\right)\right]\right\}^{-1} \tag{38}$$

Parallel with Eq. (35), the radial width α_f of the filling region is related to the average filling velocity by

$$\alpha_f = t_f r_r(360\ \mathrm{deg}) = r_r L(360\ \mathrm{deg})/\bar{v}_f \tag{39}$$

In Eq. (38), $m = \rho_{\mathrm{prop}}A_{\mathrm{HP}}L + m_{\mathrm{piston}}$. Thus, for a pressurizer having no pistons m is just the mass of propellant inside a full transfer chamber. For a system having pistons (particularly differential pistons), the mass m_{piston} of each piston can be approximated as follows. Each piston comprises a low-pressure end having a cross-sectional area A_{LP}, a thickness t_{LP}, and a mass m_{LP}, a high-pressure end having a cross-sectional area A_{HP}, a thickness t_{HP}, and a mass m_{HP}, and a connecting rod having a cross-sectional area A_{CR}, a length L, and a mass m_{CR}. The cross-sectional area A_{CR} of the connecting rod can be calculated from its material strength, with a safety factor of 2.0. The thickness of each of the ends can be approximated as 10 times the wall thickness of a sphere having the same radius. Thus,

$$\begin{aligned} m_{\mathrm{piston}} &= m_{\mathrm{HP}} + m_{\mathrm{LP}} + m_{\mathrm{CR}} \\ &= \rho_{\mathrm{piston}}A_{\mathrm{HP}}t_{\mathrm{HP}} + \rho_{\mathrm{piston}}A_{\mathrm{LP}}t_{\mathrm{LP}} + \rho_{\mathrm{piston}}A_{\mathrm{CR}}L \\ &= \rho_{\mathrm{piston}}A_{\mathrm{HP}}\left(10\frac{P_{\mathrm{HP}}r_{\mathrm{HP}}}{F_{\mathrm{all}}}\right) + \rho_{\mathrm{piston}}A_{\mathrm{LP}}\left(10\frac{P_{\mathrm{LP}}r_{\mathrm{LP}}}{F_{\mathrm{all}}}\right) \\ &\quad + \rho_{\mathrm{piston}}L\left(2\frac{P_{\mathrm{HP}}A_{\mathrm{HP}}}{F_{\mathrm{all}}}\right) \end{aligned} \tag{40}$$

Next, the radial width α_{dep} of the depressurization region can be estimated by the following approach. The radial width α_{dep} must allow sufficient depressurization time t_{dep} for the high-pressure pressurant remaining in each transfer chamber to depressurize, by exhausting via the exhaust hole; to a final pressure P_{final} at or below the pressure in the propellant tank, otherwise, propellant will not begin to flow into the transfer chamber when the transfer chamber enters the filling region. In the lower-pressure region of a cylindrical transfer chamber having length L, cross-sectional area A_{LP}, and pressure P_{LP} that is greater than exhaust pressure P_e (which can be the vacuum of space), when one end of the transfer chamber is opened to the exhaust, gas will flow out from the transfer chamber in an attempt to reach pressure equilibrium with the exhaust conditions. The force on the gas inside the transfer chamber will depend on its pressure, which drops as gas flows out from the transfer chamber. However, because gas flows out faster than temperature and pressure conditions inside the transfer chamber can equalize, the flow causes a position-dependent temperature and pressure distribution, which makes an explicit solution for t_{dep} extremely difficult. Therefore, t_{dep} can be very conservatively approximated by assuming that the final pressure P_{final} accelerates (with acceleration $a = 2L/t_{\mathrm{dep}}^2$) the initial mass m_0 of gas in the transfer chamber (as given by the Ideal Gas Law) a distance L:

$$\begin{aligned} F = P_{\mathrm{final}}A_{\mathrm{LP}} = m_0 a &= \left[\frac{P_{\mathrm{LP}}(A_{\mathrm{LP}}L)M_{\mathrm{pres}}}{R_U T_{\mathrm{pres}}}\right]\left(\frac{2L}{t_{\mathrm{dep}}^2}\right) \\ &= \left(\frac{P_{\mathrm{LP}}A_{\mathrm{LP}}M_{\mathrm{pres}}}{R_U T_{\mathrm{pres}}}\right)2\bar{v}_{\mathrm{dep}}^2 \end{aligned} \tag{41}$$

Parallel with Eq. (35), the radial width α_{dep} of the depressurization region is related to the average depressurization velocity by

$$\alpha_{\mathrm{dep}} = t_{\mathrm{dep}}r_r(360\ \mathrm{deg}) = r_r L(360\ \mathrm{deg})/\bar{v}_{\mathrm{dep}} \tag{42}$$

Next, it is axiomatic from Fig. 8 that

$$\alpha_d + \alpha_f + 2\alpha_{\mathrm{space}} + \alpha_{\mathrm{dep}} = 180\ \mathrm{deg} \tag{43}$$

Substituting Eq. (36) into Eq. (37) yields $\alpha_{\mathrm{space}} = k(360\ \mathrm{deg})\sqrt{(r_r L)}$, where k is a constant that depends only on known values of the required propellant mass flow rate, the density ρ_{prop} of the propellant, the burst pressure P_b in the lower-pressure region, the material strength F_{all} of the spindle material, and the design choice of the radius $\mathrm{r_{LP}}$ of the lower-pressure region of each transfer chamber. Substituting Eqs. (35), (37), (39), and (42) into Eq. (43) yields

$$r_r L/\bar{v}_d + r_r L/\bar{v}_f + 2k\sqrt{r_r L} + r_r L/\bar{v}_{\mathrm{dep}} = \tfrac{1}{2} \tag{44}$$

Because the average fill velocity and average depressurization velocity are known for a given application [as calculated in Eqs. (38) and (41), respectively], Eq. (44) is a simple quadratic equation that can be solved to yield $r_r L$ as a function of the average drain velocity. Substitution into Eq. (36) yields the inside radius r_1 of the chamber separators as a function of the average drain velocity, and further substitution into Eq. (32) yields the mass m_{spindle} of the spindle as a function of the average drain velocity, as shown:

$$m_{\mathrm{spindle}} = f(r_1) = f[g(r_r L)] = f\{g[h(\bar{v}_d)]\} \tag{45}$$

Having solved for m_{spindle} (as a function of average drain velocity), the next term in Eq. (29), Δm_{pres} can be found from Eqs. (11) and (12) as a function of average drain velocity. The next term in Eq. (29), the mass $\Delta m_{\mathrm{direct}}$ of pressurant lost by direct leakage, can be conservatively approximated by assuming that the pressurant leakage velocity (the velocity at which pressurant directly leaks out from between the spindle and the top chamber separator) is equal to the acoustic velocity v_a of the pressurant, which is calculated as $\sqrt{(\gamma \mathrm{RT})_{\mathrm{pres}}}$ (Ref. 12). In reality, the leakage velocity (and corresponding leakage flow) will be lower because of viscous effects. Using the Ideal Gas Law to find the density ρ_{pres} of the pressurant, $\Delta m_{\mathrm{direct}}$ can be calculated for a leakage area A_{leakage} and an engine burn time of t_{burn}:

$$\begin{aligned} \Delta m_{\mathrm{direct}} = \dot{m}_{\mathrm{direct}}t_{\mathrm{burn}} &< \rho_{\mathrm{pres}}v_a A_{\mathrm{leakage}}t_{\mathrm{burn}} \\ &= \left(\frac{P_{\mathrm{LP}}M_{\mathrm{pres}}}{R_U T_{\mathrm{pres}}}\right)\left(\gamma_{\mathrm{pres}}\frac{R_U}{M_{\mathrm{pres}}}T_{\mathrm{pres}}\right)^{\frac{1}{2}}A_{\mathrm{leakage}}t_{\mathrm{burn}} \end{aligned} \tag{46}$$

The leakage area A_{leakage} depends on the total perimeter of the pressurant entrance holes in the top chamber separator, as well as the rms width or separation w_{RMS} between the spindle and the top chamber separator:

$$A_{\mathrm{leakage}} = w_{\mathrm{RMS}}[4(r_2 - r_1) + (4\pi\alpha_d/360\ \mathrm{deg})(r_2 + r_1)] \tag{47}$$

The next term, the mass $\Delta m_{\mathrm{indirect}}$ of pressurant lost by indirect leakage, is found by first determining the volumetric propellant leakage rate Q_{propleak} from between the spindle and the bottom chamber separator and subsequently determining the mass flow rate of pressurant needed to reaccelerate this leaked (and subsequently salvaged) propellant:

$$\begin{aligned} \Delta m_{\mathrm{indirect}} = \dot{m}_{\mathrm{indirect}}t_{\mathrm{burn}} &= Q_{\mathrm{propleak}}\left(\frac{A_{\mathrm{LP}}}{A_{\mathrm{HP}}}\right)\rho_{\mathrm{pres}}t_{\mathrm{burn}} \\ &= Q_{\mathrm{propleak}}\left(\frac{A_{\mathrm{LP}}}{A_{\mathrm{HP}}}\right)\left(\frac{P_{\mathrm{LP}}M_{\mathrm{pres}}}{R_U T_{\mathrm{pres}}}\right)t_{\mathrm{burn}} \end{aligned} \tag{48}$$

The volumetric propellant leakage rate Q_{propleak} can be calculated by

$$Q_{\text{propleak}} = \frac{(A_{\text{leakage}}/w_{\text{RMS}})w_{\text{RMS}}^3 P_{\text{HP}}}{12\mu_{\text{prop}}d} \tag{49}$$

where d is the distance shown in Fig. 9 (Ref. 13). Note that every term in Eqs. (46) and (48) is dictated either by design choice (such as w_{RMS}) or a required value for a given application (such as t_{burn}), except for A_{leakage}, which depends on α_d and r_1 [as in Eq. (47)]. Because both α_d and r_1 ultimately depend on the average drain velocity, Δm_{direct} and $\Delta m_{\text{indirect}}$ can be written as a function of average drain velocity.

The last term in Eq. (29), the mass m_{ggpump} of the gas generator pump, is zero for a system utilizing differential pistons. Thus, the optimized mass $m_{\text{newLOXpump}}$ of the new LOX pump according to the present invention is found where

$$\frac{\mathrm{d}[m_{\text{newLOXpump}}(\bar{v}_d)]}{\mathrm{d}(\bar{v}_d)} = \frac{\mathrm{d}\{3m_{\text{spindle}}(\bar{v}_d) + (f_t + f_e)[\Delta m_{\text{pres}}(\bar{v}_d) + \Delta m_{\text{direct}}(\bar{v}_d) + \Delta m_{\text{indirect}}(\bar{v}_d)]\}}{\mathrm{d}(\bar{v}_d)} = 0 \tag{50}$$

For values given earlier (e.g., $f_t = 0$ and $f_e = 20.7\%$ for the Saturn V rocket, the LOX mass flow rate is 1800 kg/s with an outlet pressure of 11.0 MPa, the gas generator creates gas having $\gamma_{\text{pres}} = 1.35$, $T_{\text{pres}} = 1090$ K, and $M_{\text{pres}} = 14$ kg/kmol, etc.), the following design choices are made: the spindle is made of Al-2219 having $F_{\text{all}} = 400$ MPa and $\rho_{\text{spindle}} = 2800$ kg/m^3; the radius r_{HP} of the higher-pressure region of each transfer chamber is 1 cm (such that $A_{\text{HP}} = \pi r_{\text{HP}}^2$ and $A_{\text{LP}} = 1.2A_{\text{HP}}$); the length L is 12 cm; $\Delta P_f = 30$ psi (210 kPa); the piston is made of titanium having $F_{\text{all}} = 1.2$ GPa and $\rho_{\text{piston}} = 4460$ kg/m^3; and the distance d is 1 cm. The viscosity μ_{LOX} of LOX is about 1.89 E-4 Pa · s, and the viscosity $\mu_{\text{RP}-1}$ of RP-1 at 300 K is about 2.9 E-3 Pa · s. The only remaining parameter, the rms width w_{RMS} between the spindle and the top (or bottom) chamber separator, can be chosen as 1 mil (i.e., one thousandth of an inch, or 25.4 μm). One mil is often considered to be the lower limit of nonprecision (i.e., relatively inexpensive) machining. An rms width of a tenth of a mil or less is easily obtainable in a precision machine shop, albeit with higher expense. Based on these values, solving Eq. (50) yields a mass $m_{\text{newLOXpump}}$ of the new LOX pump of 344 kg, with values of other parameters tabulated in Table 1.

The analysis is similar for the fuel pump. However, an engineering decision must be made as to whether to use a single gas generator to provide pressurant for both the fuel and LOX pumps. Using a single gas generator simplifies the design, allowing the new LOX pump/fuel pump combination to be a true plug-and-play replacement for the F-1 turbopump (because the F-1 has a single gas generator). However, such a design requires two considerations. First, because of leakage of pressurant and propellant into the shroud of the LOX pump (as well as leakage around the pistons in the transfer chambers), the fuel-rich pressurant from the gas generator will react with the LOX, resulting in heat that must be measured and controlled. Second, because the low outlet pressure P_{LP} of the gas generator was determined in the design of the LOX pump the ratio $A_{\text{LP}}/A_{\text{HP}}$ must conform to this fixed value of P_{LP} and cannot be arbitrarily chosen as 1.2 for the new fuel pump. With these considerations in mind, a similar analysis of a new fuel pump yields a mass $m_{\text{newfuelpump}}$ of 249 kg, with values of other parameters tabulated in Table 1. The total mass of the new LOX and fuel pumps, 593 kg, is a mere 44% of the F-1 turbopump's mass of 1360 kg.

Table 1 Parameters of a new pump of the present invention having the same performance characteristics as the F-1 turbopump

Parameter	New LOX pump	New fuel pump	Total, kg
v_d	13.7 m/s	16.7 m/s	——
v_f	8.37 m/s	9.64 m/s	——
α_d	58.8 deg	54.3 deg	——
α_f	96.3 deg	94.0 deg	——
α_{space}	7.8 deg	10.6 deg	——
α_{dep}	9.4 deg	10.5 deg	——
r_{HP}	1.0 cm	1.0 cm	——
r_{LP}	1.095 cm	1.18 cm	——
r_1	20.2 cm	15.9 cm	——
r_2	40.4 cm	31.8 cm	——
L	12.0 cm	12.0 cm	——
No. transfer chambers	850	450	——
r_r	18.7 s^{-1}	21 s^{-1}	——
t_{cycle}	26.7 ms	23.8 ms	——
m_{spindle}	87.7 kg	66.3 kg	154
m_{pump}	263 kg	199 kg	462
Δm_{pump}	45.8 kg	31.8 kg	77.6
$\Delta m_{\text{leakage}}$	35.2 kg	18.2 kg	53.4
f_{direct}	70%	96%	——
f_{indirect}	30%	4%	——
m_{newpump}	344 kg	249 kg	593

An additional design consideration that has not been included in this analysis is the centrifugal pumping effect caused by rotating the spindle. The purpose of the spindle is to laterally move propellant from the low-pressure filling region to the high-pressure draining region. Energetically speaking, this lateral motion is a zero-sum transaction because the kinetic energy (in the form of dynamic pressure) imparted to the propellant by rotation of the spindle is energy that need not be imparted to the propellant by the high-pressure pressurant. Nevertheless, the greater the centrifugal pumping effect is, the larger the spindle motor must be. Therefore, the rotation rate r_r should be sufficiently modest that the majority of energy imparted to the propellant is imparted by the high-pressure pressurant. The parameters shown in Table 1 reflect such modesty. From Eq. (4), where the translational velocity v at a radius r on a cylinder rotating at r_r is given by $v = (2\pi r)r_r$, the average dynamic pressure (weighted by r) imparted to the propellant caused by the cylinder's centrifugal pumping effect is given by

$$\bar{P}_{\text{dynamic}} = \frac{\int_{r_1}^{r_2} P_{\text{dynamic}}(r) r \,\mathrm{d}r}{\int_{r_1}^{r_2} r \,\mathrm{d}r} = \frac{\int_{r_1}^{r_2} \frac{1}{2}\rho_{\text{prop}}(r_r 2\pi r)^2 r \,\mathrm{d}r}{\int_{r_1}^{r_2} r \,\mathrm{d}r} = 5\rho_{\text{prop}}(\pi r_r r_1)^2 \tag{51}$$

For the new LOX pump described in Table 1, the average dynamic pressure caused by the centrifugal effect is 804 kPa, a mere 7.3% of the pump's total outlet pressure of 11.0 MPa. Similarly, for the new fuel pump the average dynamic pressure as a result of the centrifugal effect is only 446 kPa, or 3.5% of the pump's total outlet pressure of 12.8 MPa. Even though the spindle motors for each of the pumps must be sufficient to provide 7.3 and 3.5% of their total pumping power, respectively, the total mass of pressurant fed to the pumps can be correspondingly reduced. Where the pumping power as a result of the centrifugal effect is low in comparison to the pump's total pumping power (as in the example in Table 1), the total mass of the pump system is not expected to increase significantly where the centrifugal pumping effect is included in the analysis.

C. Further Discussion of the New Pressurizer

Table 2 compares some characteristics of the three pump systems analyzed. Among the features not yet discussed are 1) reliability, 2) restartability/throttleability, 3) change in I_{sp} caused by the gas generator, and 4) cost.

Reliability

It is difficult to assess the reliability of a system without a fault-tree analysis or, better, actual test data. For example, in an official

Table 2 Parameters of competing pumps having the same performance characteristics as the F-1 turbopump

Parameter	F-1 Turbopump	Lanning Pump	New Pump
Propellant mass flow rate		1800 kg/s LOX 800 kg/s RP-1	
Outlet pressure		11.0 MPa LOX 12.8 MPa RP-1	
Combustion pressure		7.73 MPa	
Thrust @ $I_{sp} = 265$ s		6,770,000 N	
Cycle		Gas generator	
ΔI_{sp} caused by gas generator		1.8%	
Mass of pump	1360 kg	>5500 kg	462 kg
Δm_{pump}	N/A	Insignificant	77.6 kg
$\Delta m_{leakage}$	Insignificant	Insignificant	53.4 kg
Total mass of pump system	1360 kg	>5500 kg	593 kg
Thrust/weight	510	<130	1160
t_{cycle}	N/A	1 s	~25 ms
Estimated cost	$5M	<$100,000	<$100,000
Reliability	High	Higher	Highest
Restartability	No	Yes	Yes
Throttleability	No	Yes	Yes

reliability demonstration the F-1 engine was successfully tested 336 consecutive times, translating to a reliability of 99% at a confidence level of 96.6% (Ref. 5). However, in qualitatively comparing the reliabilities of the three pump systems discussed the F-1 turbopump is inherently the least reliable. The F-1 turbopump contains two centrifugal pumps, each pump having a plethora of blades connected to a common shaft. The failure of any single blade (such as by cracking) will necessarily fail—probably catastrophically—the entire pump. In contrast, in the new pump according to the present invention, the failure of one piston will not necessarily fail the entire pump. For example, should a piston unexpectedly freeze because of poor manufacturing tolerance, excessive temperature differential, or solid impurities in the propellant, the pump will continue to function, its propellant mass flow rate only slightly reduced as a result of the elimination of one of hundreds of transfer chambers. Further, a contact-based failure (i.e., a failure caused by the collision of one surface with another) is more likely to occur in the F-1 turbopump because the F-1 turbopump's high required rotational tolerances (e.g., between the rotor blades and stator structure) are more difficult to obtain than the new pump's high required flat tolerances (e.g., between the spindle and top and bottom chamber separators). The Lanning pump is likely to be more reliable than the F-1 turbopump because the only moving parts in the Lanning pump, valves, are simple in design and very reliable. However, the Lanning pump is likely to be less reliable than the new pump because, like the F-1 turbopump, a single failure is likely to fail the entire pump (because the Lanning pump will not work with any failed storage tanks).

Restartability/Throttleability

The starting sequence of the new pump is simple and does not require an additional source of gas for "spin-up," unlike turbopumps. To start the pump, the valve to the propellant tank is opened, and the spindle is slowly rotated by the spindle motor, thus filling all transfer chambers with propellant. For cryogenic propellants sufficient time is allowed for the lower portion of the spindle to cool down. Then, the valves to the gas generator and the combustion chamber are both slowly opened as the spindle motor rotates the spindle more quickly, until the valves are fully opened at the spindle's design rotation rate. Because of this simplicity, the pump is capable of multiple restarts. Further, by variably closing the valve to the gas generator and reducing the spindle's rotation rate accordingly, the propellant mass flow rate (and resulting engine thrust) may be adjusted to any arbitrary value up to 100%.

Change in Specific Impulse

The change in I_{sp} caused by the gas generator is about the same in all three pumping systems analyzed. In the F-1 engine about 3% of the propellant mass is burned in the gas generator, less than half of which is available to generate thrust by further expansion in the nozzle, yielding a net loss in I_{sp} of about 1.8%. In the new pump, as well as the Lanning pump, the total mass of pressurant (which, for a gas generator application, initially exists as liquid propellant) needed to displace the total volume of propellant at the required outlet pressure (i.e., 254 m^3 at 11.0 MPa for the LOX pump and 158 m^3 at 12.8 MPa for the fuel pump) is given by the Ideal Gas Law as 7440 kg or about 1.8% of the total propellant mass. This exhausted pressurant reduces the specific impulse by the same amount.

Cost

Estimating cost is very difficult. For example, the F-1 engine was designed and built during the Space Race, when the United States was determined to triumph at any cost. Thus, the actual marginal cost spent for each F-1 turbopump is not merely difficult to find; it simply does not exist. The cost of an F-1 turbopump, if built today, can be estimated with the following assumptions. First, the turbopump of a rocket engine typically represents about half the cost of the engine. Next, although the F-1 is almost twice as powerful as the Russian-made RD-180 (a LOX/RP-1 engine) the RD-180 far outperforms the F-1 in chamber pressure and specific impulse. In 1996, a U.S. aerospace corporation contracted to purchase 101 RD-180 engines from its Russian manufacturer at about $10M each. Assuming that a new F-1 built today would cost about the same, a new F-1 turbopump would cost about $5M. A prototype of the new pump, which will be discussed in detail later, has a mass of about 1.8 kg and cost about $2000 to build. Assuming that cost scales with mass, a 462-kg pump (as in Table 1) would cost about $500K. However, a prototype, by its very nature, costs more to produce than a large-scale mass production. Thus, the new pump described in Table 1 is expected to cost less than $100,000 in production. The Lanning pump, which is very simple, is expected to cost less than the new pump of the present invention.

The preceding design analyses have shown that the new pump according to the present invention, if applied to the F-1 engine, is lighter, simpler, less expensive, and more reliable than the original F-1 engine. However, the F-1 has a lower performance than many booster engines being used today, such as the RD-180, as used on the U.S.-made Atlas IIIB and Atlas V vehicles. Will the application of a modified F-1 engine (i.e., modified by the replacement of the turbopump with a new pump as described herein) to the booster stage of the Atlas IIIB compete with the current Atlas IIIB?

The Atlas IIIB has a total initial mass m_i of 218,600 kg, an upper-stage initial mass m_{ui} of 23,000 kg, a booster initial mass m_{bi} of 195,600 kg, a booster final mass m_{bf} (after the booster stage propellant is burned) of 13,700 kg (including the 5300 kg mass of the RD-180), a booster propellant mass $m_{bp} = m_{bi} - m_{bf} = 181{,}900$ kg, and a total final mass m_f (after the booster stage propellant is burned) $= m_{bf} + m_{ui} = 36{,}700$ kg. Assuming conservatively that the RD-180 performs at its vacuum I_{sp} of 337 s for the entire flight, Eq. (15) yields a change in velocity Δv because of the Atlas IIIB booster stage of 5890 m/s. Next, a booster stage utilizing the modified F-1 will be designed to provide the same Δv to the same upper-stage initial mass m_{ui}. Because of the F-1's lower performance and higher mass, a higher booster mass is expected. Assuming, as with the RD-180, that the F-1 performs at its vacuum I_{sp} of 305 s for the entire flight, Eq. (15) yields a total final mass m_f^* of the booster with the modified F-1 that is 16.2% of the booster propellant mass m_{bp}^* of the booster with the modified F-1. Next, the booster final mass m_{bf}^* will be approximated in terms of the booster propellant mass m_{bp}^* and known quantities by assuming that 1) the upper-stage initial mass m_{ui} remains at 23,000 kg; 2) the nonengine portion of the booster final mass m_{bf}^* (which consists primarily of tankage and structure) increases linearly with the booster propellant mass m_{bp}^*; and 3) the engine mass increases from the 5300-kg RD-180 mass to the 7700 kg mass of the modified F-1. Solving simultaneously yields a booster final mass m_{bf}^* of 20,100 kg, a booster propellant mass m_{bp}^* of 267,000 kg, and a total initial mass m_i^* of 310,100 kg. Liftoff acceleration is not reduced by using a modified F-1 in place of the RD-180; the RD-180's liftoff thrust of 3,820,000 N can accelerate a total initial mass m_i of 218,600 kg at $1.79g$, whereas the F-1's

Table 3 Features of competing boosters having the same lifting performance as the Atlas IIIB booster stage

Parameter	Current Atlas IIIB	Atlas IIIB with modified F-1
Upper-stage initial mass m_{ui}	23,000 kg	
Δv caused by booster stage	5,890 m/s	
Total initial mass m_i	218,600 kg	310,100 kg
Booster propellant mass m_{bp}	181,900 kg	267,000 kg
Booster final mass m_{bf}	13,700 kg	20,100 kg
Mass of engine	5,300 kg	7,700 kg
Liftoff thrust	3,820,000 N	Up to 6,770,000 N
Liftoff acceleration	$1.79g$	Up to $2.23g$
Approximate engine cost	\$10M	\$5M
Approximate tank/structure cost	\$3.3M	\$4.8M
Net savings	N/A	\$3.5M

liftoff thrust of 6,770,000 N can accelerate a total initial mass m_i^* of 310,100 kg at $2.23g$. The only question remaining is cost.

If 52% of the production cost of the Atlas IIIB booster stage is the propulsion system and 17% is tanks and structures,[14] and if the propulsion system is dominated by the \$10M RD-180, then tanks and structures of the booster stage cost approximately \$3.3M. By replacing the RD-180 with the modified F-1, the cost of the propulsion system drops to around \$5M (because the \$5M turbopump is replaced with the much less-expensive new pump), and the cost of tanks/structures increases proportionately with the mass of the tanks and structures to about \$4.8M. (The cost of the additional propellant is negligible.) The net savings by applying the modified F-1 to the Atlas IIIB is around \$3.5M. Table 3 compares features of these competing booster systems.

IV. Design and Test of Prototype

A prototype of the pressurizer has been designed and built by the author. Because the pump designed in the preceding section to substantially match the performance of the F-1 turbopump was too massive to build with the author's limited financial, machine shop, and laboratory resources, the prototype was designed and built to provide a propellant mass flow rate comparable to the primary reaction control system (RCS) of the space shuttle. The RCS is a simple regulated pressurant-based rocket-engine system. High-pressure helium, the pressurant, pressurizes the oxidizer (N_2O_4) tank and fuel (MMH) tank at a regulated pressure of 280 psia (1.92 MPa). The engine provides 870 lb (3870 N) of thrust with a chamber pressure of 152 psi (1.044 MPa), an I_{sp} of 280 s, and a total propellant mass flow rate of 1.41 kg/s (Ref. 15). For simplicity of testing, the prototype was designed to pump water ($\rho = 1000$ kg/m^3) at the total propellant mass flow rate of 1.41 kg/s. In a real application, however, two pumps (one for the oxidizer and one for the fuel), each having a proportionately smaller mass, would be used.

The prototype was designed and built in a simple machine shop, using a lathe and a computer numerical control (CNC) milling machine, with the limitations of such a simple shop in mind. Aluminum was chosen for most parts where possible because of its low density, high strength, and ready machinability. Most importantly, the prototype was designed and built before deriving the detailed analysis tools presented in this paper. Therefore, many parameters, such as the size of the spindle and radial widths α_d, α_f, α_{space}, and α_{dep} were chosen either arbitrarily or based on simple calculation and engineering judgment. The prototype serves to prove the concept, but is not optimized for minimum system mass.

The spindle of the prototype is shown at the top center of Fig. 11. The spindle consists of an aluminum cylinder, having an outer diameter of 2.25 in. (57.2 mm) and a length of 2.4 in. (61 mm), containing three concentric rings of 24 evenly spaced $\frac{1}{8}$in.-diam (3.2 mm-diam) transfer chambers each, as shown. Each transfer chamber contains a steel bearing ball, snugly fit inside the transfer chamber, intended to serve as the movable separator (i.e., in place of a more complicated piston). The spindle also contains steel ball bearings at each end for accommodating an axle and a steel gear for rotationally driving the spindle with an external electric motor. To contain the $\frac{1}{8}$-in. (3.2-mm) bearing balls inside the 72 transfer

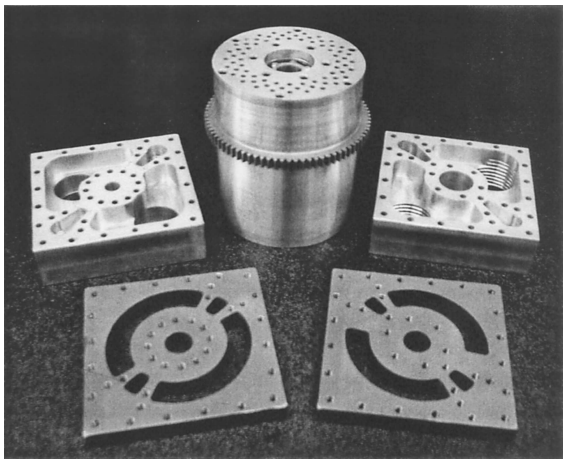

Fig. 11 Pressurizer in parts.

chambers, each end of the spindle was fitted with a brass end plate having a similar 72-hole configuration, but with each of the 72 holes having a smaller diameter to prevent the bearing balls from passing through.

The top and bottom chamber separators are shown at the bottom left and right of Fig. 11, respectively. The two chamber separators were each machined on a CNC milling machine from a 2.50-in. (63.5-mm)-square piece of ground flat steel having a thickness of 0.3125 in. (7.938 mm), and each chamber separator has two draining and filling cycles. A $\frac{1}{2}$-in. (13-mm) hole was drilled in the center of each chamber separator to accommodate a steel axle. In an attempt to minimize leakage of pressurant and propellant from the draining region, the radial width α_d of each draining region was chosen to be very small—only 15 deg. The radial width α_{space} of each space/separation region was chosen as 10 deg because it is substantially greater than the arc length of a transfer chamber diameter in the inner ring of holes, which is calculated as 7.2 deg. The radial width α_{dep} of each depressurization region was conservatively chosen as 20 deg. Finally, the remaining 125 deg of each 180-deg cycle was assigned as the radial width α_f of each filling region.

For these values exactly six transfer chambers, each having an inside cross-sectional area A_c determined by their diameter of $\frac{1}{8}$ in. (3.2 mm), are available to drain at any given time. Thus, the average drain velocity necessary to ensure a propellant mass flow rate of 1.41 kg/s is 29.5 m/s, as calculated from Eq. (3). The drain time t_d of 2.1 ms and the required rotation rate r_r of 20.2 s^{-1} (1200 rpm) are calculated from Eq. (35). The pressure drop ΔP_d across the draining region necessary to achieve the required average drain velocity inside each transfer chamber is 360 psi (2.47 MPa), as given by Eq. (11), where the mass m includes the mass $\rho_{water} A_c L$ of the propellant (water) inside the transfer chamber and the mass m_{bb} of the steel bearing ball separator.

Next, two plumbing plates (shown top, Fig. 11), one for each chamber separator, were machined from aluminum and bolted to the chamber separators. The top plumbing plate was designed to channel flow of high-pressure pressurant to the two pressurant entrance holes of the top chamber separator via two female $\frac{1}{8}$-in. (3.2-mm) standard pipe threads and to channel flow of low-pressure exhaust from the two pressurant exhaust holes via two female $\frac{1}{2}$-in. (13-mm) standard pipe threads. Similarly, the bottom plumbing plate was designed to channel flow of high-pressure propellant from the two propellant exit holes of the bottom chamber separator via two female $\frac{1}{8}$-in. (3.2-mm) standard pipe threads and to channel flow of low-pressure propellant to the two propellant entrance holes via two female $\frac{1}{2}$-in. (13-mm) standard pipe threads.

Next, the five parts were assembled between two longitudinal aluminum plates as shown in Fig. 12, with a steel axle passing from the center hole in the top chamber separator, through the two ball bearings in the spindle, to the center hole in the bottom chamber separator. A steel bolt (not shown) was rotatably connected between the longitudinal aluminum plates and the top plumbing plate and configured so that the distance between the chamber separators and the

Fig. 12 Assembled pressurizer.

spindle there between—and therefore the width w_{RMS} of the leakage path—could be adjusted by adjusting the tightness of the bolt. Finally, a 250-W electric motor (not shown) was attached to the prototype and configured to rotate the spindle with respect to the chamber separators by engaging with the steel gear teeth on the spindle.

A lapping abrasive was then chosen to decrease the rms separation w_{RMS} between the spindle and chamber separators to below the lower limit of nonprecision machining of one mil (25.4 μm). A lapping or liquid abrasive (which comprises tiny particles, such as diamond, alumina, or silicon dioxide, that are harder than the materials being lapped) pulverizes the unwanted peaks of rough running surfaces until the rms roughness of the running surfaces is on the order of the rms diameter of the particles in the lapping abrasive. A 1000-grit [corresponding to an rms particle diameter of around 350 μin. (9 μm)] oil-based SiO_2 lapping abrasive was applied to both sets of the prototype's running surfaces (i.e., between the spindle and the top chamber separator and between the spindle and the bottom chamber separator) and the spindle was spun at around 500 rpm for several hours. A leakage test of the pressurant was later performed, which demonstrated a leakage rate of about half that calculated for a true rms separation of one mil (25.4 μm). Although some measures were taken to reduce leakage, the prototype was designed only for proving the concept, not optimization. In a future test the running surfaces could be further lapped to a lower rms roughness; lapping abrasives are readily available that create finishes having rms roughnesses as low as 1 μin. (25 nm).

The prototype, once designed, was built in about 50 hours of machining time. At \$40/hr for nonprecision work, the prototype cost about \$2000. The mass of the spindle is about 0.60 kg, and the mass of the entire prototype is about 1.80 kg.

The test apparati consisted of a test pressurant tank, a test propellant tank, a tank of pressurized N_2, and the appropriate valves and plumbing. Because of its ready availability and low expense, PVC piping having a relatively low maximum working pressure was chosen as the test pressurant tank. Even though the pressure drop ΔP_d across the draining region necessary to sustain the required average drain velocity is 360 psi (2.47 MPa), as calculated earlier, the PVC test pressurant tank was pressurized with N_2 to a regulated pressure of only 280 psi (1.92 MPa). The test propellant tank, also made of PVC, was filled with water (to simulate a propellant having a specific gravity of 1) and regulated to 34 psi (0.23 MPa) with N_2. The prototype was then tested. Because of the fluid bearing effect caused by pressurant and propellant leakage, the spindle consistently spun well above the 1200 rpm design rotation rate. (Because of a photo-tachometer failure, the exact rotation rate is unknown; it could be as high as 6000 rpm.)

After several successful tests the pressurizer in the final test pumped 9.78 kg of water in 40 s, yielding a mass pumping rate of 0.24 kg/s.

The fact that 0.24 kg/s is almost six times less than the propellant mass flow rate in the RCS can be explained as follows. First, the mass flow rate of pressurant from the test pressurant tank was far greater than the nitrogen regulator could sustain at 280 psi (1.92 MPa). Thus, the pressurant tank pressure, during steady-state operation, was around 220 psi (1.51 MPa), about 61% of the 360 psi (2.47 MPa) (calculated earlier) required to sustain the RCS's 1.41 kg/s mass flow rate. Second, pressurant leakage might have caused a further pressure drop that reduced ΔP_d to below 220 psi (1.51 MPa). Finally, the mass flow rate was reduced by a rotation rate far in excess of the design rotation rate of 1200 rpm. For example, recognizing that $t_d = \alpha_d/(r_r \times 360 \text{ deg})$, and choosing $P_1 - P_2 = 1.51$ MPa and $r_r = 80 \text{ s}^{-1}$ (4800 rpm), Eq. (9) yields an average drain velocity inside each transfer chamber of 5.0 m/s, which corresponds to a propellant mass flow rate of 0.24 kg/s from Eq. (3).

The pressurizer leaked about 0.022 kg/s of water, for an indirect leakage rate of about 10%. Because the test was performed with an rms separation between the running surfaces of about 500 μin. (13 μm) [instead of a preferred 50 μin. (1.3 μm) or less], this leakage rate can easily be reduced by more than an order of magnitude in future tests.

V. Conclusion

A new technology has been invented that will likely yield substantial mass and cost savings if applied to preexisting turbopump-based rocket-engine systems. A prototype has been independently designed and built that successfully proves the concept. Further testing and development of the technology have been interrupted for the purpose of soliciting interest in and funding for this technology. For further information, please contact the author.

Acknowledgments

Fred Cote, Manuel Martinez-Sanchez, James Robertson, Carl Dietrich, Andrew Heafitz, and the Massachusetts Institute of Technology Rocket Team are sincerely thanked for their help with this research. I would also like to thank my parents, Fred and Lynne, and my sister, Dani, for their continual support.

References

[1]Humble, R. W., Larson, W. J., and Henry, G. N., *Space Propulsion Analysis and Design*, McGraw–Hill, New York, 1995, p. 272.

[2]Sobey, A., "Fluid Pressurizing System," U.S. Patent No. 3,213, 804, 26 Oct. 1965.

[3]Lanning, M. E., and Blackmon, J. B., Jr., "Reciprocating Feed System for Fluids," U.S. Patent No. 6,314,978, 13 Nov. 2001.

[4]Harrington, S., "Pistonless Dual Chamber Rocket Fuel Pump: Testing and Performance," AIAA Paper 2003-4479, July 2003.

[5]Biggs, B., "F-1: The No-Frills Giant," *Threshold*, No. 8, Spring 1992, pp. 20–31.

[6]Humble, R. W., Larson, W. J., and Henry, G. N., *Space Propulsion Analysis and Design*, McGraw–Hill, New York, 1995, pp. 707, 708.

[7]Isakowitz, S. J., *International Reference Guide to Space Launch Systems*, AIAA, Washington, D.C., 1991, p. 292.

[8]Humble, R. W., Larson, W. J., and Henry, G. N., *Space Propulsion Analysis and Design*, McGraw–Hill, New York, 1995, p. 13.

[9]Knight, A. F., "Pressurizer for a Rocket Engine," U.S. Patent No. 6,499,288, 31 Dec. 2002.

[10]Knight, A. F., "The Race for Low-Cost Launch Vehicles: A New Rocket Engine Design," *High Power Rocketry*, Vol. 33, No. 3, 2002, pp. 7–10, 27.

[11]Humble, R. W., Larson, W. J., and Henry, G. N., *Space Propulsion Analysis and Design*, McGraw–Hill, New York, 1995, pp. 270, 271.

[12]Humble, R. W., Larson, W. J., and Henry, G. N., *Space Propulsion Analysis and Design*, McGraw–Hill, New York, 1995, p. 100.

[13]Cundiff, J. S., *Fluid Power Circuits and Controls*, CRC Press, Boca Raton, FL, 2002, p. 45.

[14]Hammond, W. E., *Space Transportation: A Systems Approach to Analysis and Design*, AIAA, Reston, VA, 1999, p. 410.

[15]Sutton, G. P., and Biblarz, O., *Rocket Propulsion Elements*, 7th ed., Wiley, New York, 2001, p. 210.